Data-dependent orthogonal polynomials on generalized circles

Automatica 131 (2021) 109709

Contents lists available at ScienceDirect

Automatica

journal homepage: www.elsevier.com/locate/automatica

Data-dependent orthogonal polynomials on generalized circles: A unified approach applied to δ-domain identification ☆

Robbert Voorhoeve, Tom Oomen *

Eindhoven University of Technology, Department of Mechanical Engineering, Control Systems Technology group, The Netherlands

ARTICLE INFO

Article history:
Received 24 October 2019
Received in revised form 12 January 2021
Accepted 1 May 2021
Available online 7 June 2021

ABSTRACT

The performance of algorithms in system identification and control, depends on their implementation in finite-precision arithmetic. The aim of this paper is to develop a unified approach for numerically reliable system identification that combines the numerical advantages of data-dependent orthogonal polynomials and the discrete-time δ-domain parametrization. In this paper, earlier results for discrete orthogonal polynomials on the real-line and the unit-circle are generalized to obtain an approach for the construction of orthogonal polynomials on generalized circles in the complex plane. This enables the formulation of a unified framework for the numerically reliable identification of systems expressed in the δ-domain, as well as in the traditional Laplace and Z-domains. An example is presented which shows the significant numerical advantages of the δ-domain approach for the identification of fast-sampled systems.

1. Introduction

Numerically robust and accurate implementation of algorithms used in system identification and control is essential for their successful application (Datta, 2004; Varga, 2004). This numerical aspect becomes more relevant and challenging as the system complexity increases (Benner, 2004; Oomen et al., 2014). Several approaches that address the encountered numerical issues have been proposed. In particular, the use of the discrete δ-domain as opposed to the classical Z-domain addresses several numerical issues in digital control implementations with fast sampling (Goodwin, Middleton, & Poor, 1992). In the present paper, numerically reliable identification is investigated and a unified framework is presented that, as a special case, enables the numerically reliable identification of system models expressed in the discrete δ-domain.

In parametric system identification, the central computational step typically involves solving a linear least squares problem, which often is severely ill-conditioned (Levy, 1959; Ninness & Hjalmarsson, 2001; Sanathanan & Koerner, 1963; Voorhoeve, van Rietschoten, Geerardyn, & Oomen, 2015). Several partial solutions to this conditioning problem have been proposed, including the use of frequency scaling (Pintelon & Kollár, 2005), the use of orthonormal bases such as Chebyshev polynomials, or Laguerre or Kautz filters (Ninness & Hjalmarsson, 2001; Wahlberg & Mäkilä, 1996), and the use of certain rational basis functions (Gilson, Welsh, & Garnier, 2018; Gustavsen & Semlyen, 1999; Welsh & Goodwin, 2003). Another recent development is the use of polynomial basis functions, which are orthogonal with respect to a discrete data-dependent inner product (Bultheel, Barel, Rolain, & Pintelon, 2005; van Herpen, Oomen, & Steinbuch, 2014; Rolain, Pintelon, Xu, & Vold, 1995). Using these data-dependent orthonormal polynomials optimal numerical conditioning, i.e., a condition number $\kappa = 1$, can be achieved (Bultheel et al., 2005; van Herpen et al., 2014). Thereby essentially solving the main numerical bottlenecks and enabling the identification of highly complex systems (Pintelon, Rolain, Bultheel, & Barel, 2004; Voorhoeve, de Rozario, & Oomen, 2016). Efficient algorithms, which are linear in the data and the polynomial degree, i.e., $\mathcal{O}(mn)$, exist for the construction of these data-dependent orthogonal polynomials for continuous time systems, i.e., for $s = j\omega$, with nodes on the imaginary axis (Gragg & Harrod, 1984); and for discrete time systems, i.e., for $z = e^{j\omega T_s}$, with nodes on the unit circle (Ammar, Gragg, & Reichel, 1991).

Another improvement of numerical aspect for algorithms in system identification and control can be achieved by replacing the traditional forward-shift operator, q, with the forward-difference operator, δ (Goodwin, Leal, Mayne, & Middleton, 1986; Middleton

☆ This research is supported by the TU/e impulse program in collaboration with ASML Research and is part of the research programme VIDI with project number 15698, financed by the Netherlands Organization for Scientific Research (NWO). The material in this paper was partially presented at the 57th IEEE Conference on Decision and Control, December 17–19, 2018, Miami Beach, Florida, USA. This paper was recommended for publication in revised form by Associate Editor Juan C Aguero under the direction of Editor Torsten Söderström.

* Corresponding author.
E-mail addresses: r.j.voorhoeve@gmail.com (R. Voorhoeve), t.a.e.oomen@tue.nl (T. Oomen).

https://doi.org/10.1016/j.automatica.2021.109709

& Goodwin, 1986). The δ-operator transparently connects models in the discrete time domain and the continuous time domain, as the continuous time model parameters are recovered in the limit case for the sample time tending to zero (Goodwin et al., 1986). Furthermore, using the δ-operator instead of the shift operator often leads to improved numerical performance when considering finite-word-length effects (Middleton & Goodwin, 1986). These advantages have been shown to be especially relevant for systems with fast sampling (Goodwin et al., 1992; Li & Gevers, 1993), i.e., where the sampling frequency is significantly higher than the dominant system dynamics, which is often the case in identification for control (Gevers & Li, 1993). In controller synthesis, a δ-domain parametrization has also shown to yield substantial numerical advantages (Collins & Song, 1999; Goodwin, Graebe, & Salgado, 2000; Suchomski, 2001; Yang, Xia, Shi, & Zhao, 2012).

Although data-dependent orthonormal polynomials have been shown to provide significant numerical advantages in system identification, at present their advantages are limited due to a numerical loss of accuracy in other essential computation steps. The aim of this paper is to develop a unified approach for numerically reliable system identification that combines the numerical advantages of data-dependent orthogonal polynomials and the discrete-time δ-domain parametrization. The main contributions of this paper are the following.

(1) A theoretical framework and efficient construction algorithm for polynomials that are orthogonal with respect to discrete measures supported on generalized circles in the complex plane, expanding on earlier results for measures supported on the real-line, and the unit circle.
(2) A unified framework for numerically reliable system identification, including identification in the δ-domain, Z-domain, and Laplace domain.
(3) An example revealing the superior numerical performance of the δ-domain approach over the Z-domain approaches for fast-sampled systems.

In earlier approaches, e.g., Bultheel and Barel (1995) and Bultheel et al. (2005), efficient construction of data-dependent orthogonal polynomials is limited either to the case of measures supported on the real or imaginary line (Gragg & Harrod, 1984) or on the unit circle (Ammar et al., 1991). In contrast, for the relevant case of the δ operator, the nodes lie on a circle in the complex plane for which the existing efficient solutions do not apply. The specific δ-domain case is considered in Voorhoeve and Oomen (2018). In the present paper, the preliminary results in Voorhoeve and Oomen (2018) are extended by considering the construction of orthogonal polynomials from spectral data on generalized circles in the complex plane. This leads to a unified framework where identification in Laplace domain, Z-domain, and δ-domain can be considered as special cases and can be solved with a single algorithm.

The outline of this paper is as follows. In Section 2, the problem of numerically reliable identification of fast sampled systems is formulated. Section 3 provides a concise overview of the theory of data-dependent orthogonal polynomials. In Section 4, the theory and construction algorithm for data-dependent orthogonal polynomials on generalized circles in the complex plane are considered, constituting contribution 1 of this paper. In Section 5, this algorithm is used to obtain a unified framework for numerically reliable system identification, constituting contribution 2 of this paper. In Section 6, the results for a simulation example are presented, showing the superior performance of the δ-domain approach compared to the Z-domain approaches for fast-sampled systems, constituting contribution 3 of this paper. In Section 7, conclusions and an outlook on ongoing work are given.

2. Problem formulation

The problem considered in this paper is that of numerically reliable frequency-domain identification of linear systems with fast sampling. First, the problem of frequency domain system identification is defined. Second, numerically reliable identification is considered. Last, the numerical challenges for fast-sampled systems are highlighted and the advantages of the proposed δ-domain approach are illustrated, leading to the formulation of the considered problem of numerically reliable identification in the δ-domain.

2.1. Frequency domain system identification

In system identification, a physical process is considered which is observed using a digital measurement environment. The goal in system identification is to estimate an appropriate system model, $\hat{G}(\xi)$, describing the relevant behavior of this physical process. In frequency domain identification this is done using frequency domain input–output data of the system. To facilitate the presentation, identification of single-input single-output (SISO) systems is considered, the extension to multiple-input multiple-output (MIMO) systems follows along similar lines as in, e.g., Pintelon et al. (2004) and Voorhoeve et al. (2016).

In this paper, linear time invariant (LTI) systems are considered, represented by real-rational transfer functions, $\hat{G}(\xi) \in \mathcal{R}$. Here, ξ, is an indeterminate frequency variable which depends on the identification domain. For continuous-time modeling the Laplace domain, where $\xi = s = j\omega$, is traditionally used, while discrete-time modeling is generally performed in the Z-domain, with $\xi = z = e^{j\omega T_s}$. Here ω is the frequency variable and T_s is the sampling time of the digital measurement environment. The model $\hat{G}(\xi)$ is parametrized as

$$\hat{G}(\xi, \theta) = \frac{\hat{n}(\xi, \theta)}{\hat{d}(\xi, \theta)}, \tag{1}$$

where $\hat{n}(\xi, \theta)$, $\hat{d}(\xi, \theta) \in \mathbb{R}[\xi]$, which are linearly parametrized with respect to a set of polynomial basis functions $\{\phi_j(\xi)\}_{j=0}^{n}$, i.e.,

$$\begin{bmatrix} \hat{d}(\xi, \theta) \\ \hat{n}(\xi, \theta) \end{bmatrix} = \begin{bmatrix} \phi_0(\xi) & \phi_1(\xi) & \cdots & \phi_n(\xi) \end{bmatrix} \theta, \tag{2}$$

with $\theta \in \mathbb{R}^{n_\theta \times 1}$ and $\phi_j(\xi) \in \mathbb{R}^{2\times 1}[\xi]$.

The optimal model within this parametrization is then selected by minimizing a suitable error criterion, e.g., $\hat{G}_{\text{opt}}(\xi) = \hat{G}(\xi, \theta_{\text{opt}})$, where

$$\theta_{\text{opt}} = \arg\min_{\theta} \sum_{i=1}^{m} \left| \tilde{w}_i \left(\tilde{G}(\xi_i) - \hat{G}(\xi_i, \theta) \right) \right|^2, \tag{3}$$

and where $\tilde{G}(\xi_i)$ is the identified FRF of the system. This weighted least squares criterion encompasses many relevant criteria in identification, including sample maximum likelihood identification (Pintelon & Schoukens, 2012, Section 12.3) and control-relevant identification (Oomen et al., 2014). Solving (3) generally involves solving a nonlinear optimization problem due to the rational parametrization of $\hat{G}(\xi)$. Indeed, rewriting (3) yields

$$\theta_{\text{opt}} = \arg\min_{\theta} \sum_{i=1}^{m} \left| \frac{\tilde{w}_i}{\hat{d}(\xi_i, \theta)} \begin{bmatrix} \tilde{G}(\xi_i) & -1 \end{bmatrix} \begin{bmatrix} \hat{d}(\xi_i, \theta) \\ \hat{n}(\xi_i, \theta) \end{bmatrix} \right|^2. \tag{4}$$

The form (4) facilitates the derivation of several common solution algorithms.

First, the solution to (4) can be approximated by solving the following linear least squares problem.

Algorithm 1 (*Linear Least Squares, Levy, 1959; Pintelon & Schoukens, 2012, Section 9.8.2*)**.** Given $\tilde{w}_{i,\mathrm{lin}}$, compute

$$\theta_{\mathrm{lin}} = \arg\min_{\theta} \sum_{i=1}^{m} \left| \tilde{w}_{i,\mathrm{lin}} \begin{bmatrix} \tilde{G}(\xi_i) & -1 \end{bmatrix} \begin{bmatrix} \hat{d}(\xi_i, \theta) \\ \hat{n}(\xi_i, \theta) \end{bmatrix} \right|^2 . \tag{5}$$

In (5), $\tilde{w}_{i,\mathrm{lin}}$ replaces the nonlinear term $\frac{\tilde{w}_i}{\hat{d}(\xi_i,\theta)}$, which is present in the original problem (4), rendering (5) linear in the parameters θ. If $\tilde{w}_{i,\mathrm{lin}} = \tilde{w}_i$, the standard linear least squares solution of Levy (1959) is obtained. If an appropriate estimate for the denominator polynomial $\hat{d}(\xi_i)$ is available, its inverse can be used to weight the linearized problem, aiming to address the original problem, (4). Such an estimate for the denominator can be obtained by iteratively solving a sequence of linear least squares problems. This approach is known as the Sanathanan–Koerner (SK) algorithm.

Algorithm 2 (*Sanathanan–Koerner, Sanathanan & Koerner, 1963; van Herpen et al., 2014, Algorithm I; Pintelon & Schoukens, 2012, Section 9.8.3*)**.** Given $\theta^{\langle 0 \rangle}$, compute for $l = 1, 2, \ldots$

$$\theta_{\mathrm{SK}}^{\langle l \rangle} = \arg\min_{\theta} \sum_{i=1}^{m} \left| \frac{\tilde{w}_i}{\hat{d}(\xi_i, \theta^{\langle l-1 \rangle})} \begin{bmatrix} \tilde{G}(\xi_i) & -1 \end{bmatrix} \begin{bmatrix} \hat{d}(\xi_i, \theta) \\ \hat{n}(\xi_i, \theta) \end{bmatrix} \right|^2 . \tag{6}$$

Alternatively, gradient-based optimization methods can be used such as the Gauss–Newton algorithm or the closely related Levenberg–Marquardt algorithm. These gradient-based algorithms enable monotonic convergence to a local minimum of the non-linear cost function, yielding favorable results when an initial estimate of sufficient quality is available. Using a similar notation as in (6), the Gauss–Newton algorithm for the optimization of (3) is as follows.

Algorithm 3 (*Gauss–Newton, Bayard, 1994*)**.** Given $\theta^{\langle 0 \rangle}$, compute for $l = 1, 2, \ldots$

$$\theta_{\mathrm{GN}}^{\langle l \rangle} = \theta^{\langle l-1 \rangle} + \arg\min_{\Delta\theta} \sum_{i=1}^{m} \left| J(\xi_i, \theta^{\langle l-1 \rangle}) \Delta\theta + \varepsilon(\xi_i, \theta^{\langle l-1 \rangle}) \right|^2 , \tag{7}$$

with

$$J(\xi_i, \theta^{\langle l \rangle})\, \Delta\theta = \frac{\tilde{w}_i}{\hat{d}(\xi_i, \theta^{\langle l \rangle})} \begin{bmatrix} \hat{G}(\xi_i, \theta^{\langle l \rangle}) & -1 \end{bmatrix} \begin{bmatrix} \hat{d}(\xi_i, \Delta\theta) \\ \hat{n}(\xi_i, \Delta\theta) \end{bmatrix} , \tag{8}$$

$$\varepsilon(\xi_i, \theta^{\langle l \rangle}) = \tilde{w}_i \left(\tilde{G}(\xi_i) - \hat{G}(\xi_i, \theta^{\langle l \rangle}) \right) . \tag{9}$$

In these solution algorithms, i.e., in (5), (6), (7), but also in many other identification algorithms, such as the Least-Squares Complex Frequency-domain estimator (Van der Auweraer, Guillaume, Verboven, & Vanlanduit, 2001) or Iterative Quadratic Maximum Likelihood (Pintelon & Schoukens, 2012, Section 9.12), the essential problem being solved is a weighted polynomial least squares problem. This problem can be expressed in the general form,

$$\min_{\theta} \| \boldsymbol{w} f(\boldsymbol{\xi}, \theta) \|_2^2 , \tag{10}$$

with

$$\boldsymbol{w} = [w_1^T,\ w_2^T, \ldots,\ w_m^T]^T \tag{11}$$

$$\boldsymbol{\xi} = [\xi_1,\ \xi_2, \ldots,\ \xi_m]^T , \tag{12}$$

and where

$$\| \boldsymbol{w} f(\boldsymbol{\xi},\ \theta) \|_2^2 := \sum_{i=1}^{m} f(\xi_i,\ \theta)^H w_i^H\ w_i f(\xi_i,\ \theta) , \tag{13}$$

with

$$f(\xi_i, \theta) = p(\xi_i, \theta) - y_i , \tag{14}$$

where y_i is determined by the problem data and the parameter constraints. Therefore, the problem that is considered in this paper is of this form, where for clarity only the scalar polynomial case is considered, i.e., $p(\xi,\ \theta) \in \mathbb{R}[\xi]$. Extensions to the vector polynomial case, i.e., $p(\xi,\ \theta) \in \mathbb{R}^n[\xi]$ are discussed in Section 7.

2.2. Numerically reliable identification

Solving the polynomial least-squares problem, (10), is equivalent to determining the least-squares solution to

$$W \Phi_n \theta = W \boldsymbol{y} , \tag{15}$$

with

$$W = \mathrm{diag}(w_1,\ w_2, \ldots,\ w_m) , \tag{16}$$

$$\boldsymbol{y} = [y_1,\ y_2, \ldots,\ y_m]^T , \tag{17}$$

$$\Phi_n = \begin{bmatrix} \phi_0(\xi_1) & \phi_1(\xi_1) & \cdots & \phi_n(\xi_1) \\ \phi_0(\xi_2) & \phi_1(\xi_2) & \cdots & \phi_n(\xi_2) \\ \vdots & \vdots & & \vdots \\ \phi_0(\xi_m) & \phi_1(\xi_m) & \cdots & \phi_n(\xi_m) \end{bmatrix} , \tag{18}$$

which depends on the weights in W and the basis functions in Φ_n. The key observation is that the matrix $W\Phi_n$ in (15) can be severely ill-conditioned depending on the choice of basis functions. Indeed, it is well-known that if a monomial basis, $\phi_j(\xi) = \xi^j$, is used, then Φ_n is a Vandermonde matrix, i.e.,

$$\Phi_{\mathrm{n}}^{\mathrm{mon}} = \begin{bmatrix} 1 & \xi_1 & \xi_1^2 & \cdots & \xi_1^n \\ 1 & \xi_2 & \xi_2^2 & \cdots & \xi_2^n \\ \vdots & \vdots & \vdots & & \vdots \\ 1 & \xi_m & \xi_m^2 & \cdots & \xi_m^n \end{bmatrix} , \tag{19}$$

which is often ill-conditioned, deteriorating the performance of the identification algorithms (van Herpen et al., 2014).

Several approaches have been proposed in literature to mitigate this conditioning problem (Gilson et al., 2018; Gustavsen & Semlyen, 1999; Ninness & Hjalmarsson, 2001; Pintelon & Kollár, 2005; Wahlberg & Mäkilä, 1996; Welsh & Goodwin, 2003), confirming that this is an important aspect in frequency domain system identification. The approaches in Gilson et al. (2018), Gustavsen and Semlyen (1999), Ninness and Hjalmarsson (2001), Wahlberg and Mäkilä (1996) and Welsh and Goodwin (2003) focus on a change of basis functions to obtain a Φ-matrix which has better numerical properties than the Vandermonde matrix in (19). However, this does not guarantee an improvement in the conditioning of $W\Phi$, which is the relevant problem matrix for solving (15). To guarantee that $W\Phi$ is well-conditioned, the problem data, as contained in W, needs to be taken into account in the choice of basis functions, i.e., the basis functions should be data-dependent. A key result in, e.g., Bultheel and Barel (1995) and Bultheel et al. (2005), shows that optimal conditioning of $W\Phi$ can indeed be achieved using a set of polynomials which are orthonormal with respect to a judiciously chosen data-based inner product.

Being able to achieve optimal conditioning of the problem matrix $W\Phi$ is an important step towards obtaining a numerically reliable identification approach. However, other computational steps involved in the identification algorithm should also be performed numerically accurate. For systems with fast sampling inherent numerical challenges exist which need to be addressed.

2.3. Numerical challenges for fast-sampled systems: motivation for a δ-domain formulation

In the identification problem as stated in Section 2.1, ξ in (1) still remains to be specified. Typically, the Laplace domain, $\xi = s$,

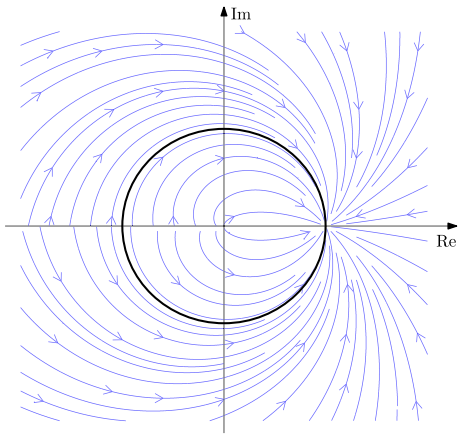

Fig. 1. Streamlines for the vector field $dz/df_s \propto -z\ln(z)$ showing the attraction of point $z = 1$ as the sampling frequency increases.

is used when the system is in continuous time, whereas the Z-domain, $\xi = z$, is used when the system is in discrete time. For both these cases, efficient algorithms exist to construct the data-dependent orthogonal polynomials used in numerically reliable identification, as described in Section 2.2. However, when the sampling frequency of the digital measurement environment is fast relative to the dominant dynamics of the underlying physical process, the discrete Z-domain description is known to suffer from numerical issues.

To analyze the numerical issues that arise for fast-sampled systems in the Z-domain, the derivative of the complex variable $z = e^{s/f_s}$ with respect to the sampling frequency $f_s = 1/T_s$ is considered,

$$\frac{dz}{df_s} = \frac{de^{s/f_s}}{df_s} = -\frac{e^{s/f_s}\, s}{f_s^2} = -\frac{z\ln(z)}{f_s} \propto -z\ln(z)\,, \tag{20}$$

where $s = f_s \ln(z)$ is used in the third step and where $\propto$ denotes proportionality. Streamlines for the vector field $-z\ln(z)$ are plotted in the complex plane in Fig. 1. This figure clearly shows that all streamlines converge to the point $z = 1$. For fast-sampled systems this essentially means that the poles describing the system dynamics will become concentrated near the point $z = 1$.

This concentration around $z = 1$ leads to a numerical loss of significance in finite precision arithmetic since a large part of the available finite wordlength is used to store this "unity part" of the relevant parameters, which does not contain any system information. Also, cancellation errors occur when parameters with values that are only marginally different from 1 are subtracted from one another.

As an alternative to the Z-domain description, the discrete-time system can be represented in the δ-domain where the δ-operator is used instead of the shift operator q, where

$$\delta = \frac{q-1}{T_s}\,, \tag{21}$$

and the corresponding transform variable,

$$\xi_\delta = \frac{z-1}{T_s}\,. \tag{22}$$

The main numerical advantage of this δ-domain description is that it shifts the point $z = 1$ to the origin, solving the associated loss of significance problems. Additionally, the δ operator intuitively connects the discrete and continuous time domains as for a differentiable function $x(t)$

$$\lim_{T_s\to 0} \delta x(t) = \lim_{T_s\to 0} \frac{x(t+T_s)-x(t)}{T_s} = \frac{dx}{dt}\,, \tag{23}$$

meaning that as the sampling frequency increases the δ-domain parameters converge to the continuous time parameters. This provides insight and gives confidence that even for sampling time approaching zero the discrete-time description in the δ-domain remains well behaved.

The δ-domain representation often improves numerical aspects. However, fast construction of data-dependent orthonormal polynomials as used in, e.g., Bultheel and Barel (1995) and Bultheel et al. (2005), has not been investigated for δ-domain identification. In this paper, the problem of efficient construction of data-dependent orthonormal polynomials for numerically reliable δ-domain identification is considered.

3. Data-dependent orthonormal polynomials

In this section, orthogonal polynomials with respect to a data-dependent discrete inner product are defined. The study of orthogonal polynomials is a well-developed and active field, see, e.g., Gautschi (2004), Simon (2005) and Szegö (1939). In this paper, the focus is on discrete inner products in contrast to the commonly considered continuous inner products involving integrals. In addition, an arbitrary weighting is used in the inner product, see also Vandebril, Van Barel, and Mastronardi (2008a, Chapter 12) for details on such forms, and van Herpen, Bosgra, and Oomen (2016) for related indefinite and asymmetric forms.

In Section 3.1, discrete orthogonal polynomials are defined. Next, a Hessenberg recurrence relation for this set of polynomials is considered in Section 3.2, and the inverse eigenvalue problem linking the Hessenberg-recurrence matrix to the problem data is established in Section 3.3. Next, an algorithm for solving this inverse eigenvalue problem is considered in Section 3.4, as well as the special cases when all the nodes lie on the real-line, the imaginary-axis or the unit circle in Section 3.5. In this section and in Section 4, the general case of polynomials with complex coefficients is considered. In Section 5, the real-polynomial case, which is relevant for identification, is considered.

3.1. Discrete orthogonal polynomials

Consider the set of polynomials $\{\phi_j(\xi)\}_{j=0}^{k}$ where $\phi_j(\xi) \in \mathbb{C}[\xi]$, and $\deg \phi_j(\xi) = j$, which is orthogonal with respect to a discrete inner-product defined by the nodes $\xi_1, \xi_2, \ldots, \xi_m \in \mathbb{C}$ and weights $w_1, w_2, \ldots, w_m \in \mathbb{C}$, i.e.,

$$\langle \phi_p, \phi_q \rangle = \sum_{i=1}^{m} \left(w_i\, \phi_p(\xi_i)\right)^* w_i\, \phi_q(\xi_i) = c_p \delta_{pq}\,, \tag{24}$$

with $c_p \in \mathbb{R}^+$, and where δ_{pq} is the Kronecker delta function, and x^* denotes the complex conjugate of x. In matrix form (24) is given by

$$\Phi_k^H W^H W \Phi_k = D, \tag{25}$$

with W as defined in (16), Φ_k as defined in (18) but with k columns instead of n, and where $D = \operatorname{diag}(c_0, c_1, \ldots, c_k)$. Furthermore, the polynomials ϕ_j are normalized such that $c_j = 1\ \forall\ c_j \neq 0,\ j = 0, \ldots, k$.

Without loss of generality, it is assumed that $w_i \neq 0\ \forall\ i$. Indeed, if $w_i = 0$, the corresponding node-weight pair can be removed from (24) without altering the inner product. Therefore, $\operatorname{rank}(W) = m$ and consequently $\operatorname{rank}(D) \leq m$, due to (25). This means there are at most m polynomials for which $c_j \neq 0$. In fact, under the assumption that there are no duplicate nodes, the first m polynomials are the ones for which $c_j \neq 0$. This follows from the fact that the square matrix Φ_{m-1}, containing these first m polynomials, is bijectively related to the square Vandermonde matrix defined by the nodes ξ_i, which has a nonzero determinant

as long as all the nodes are distinct (Gautschi, 1983). Therefore, $c_j = 1$ for $j = 0, \ldots, m-1$, i.e.,

$$\Phi_{m-1}^H W^H W \Phi_{m-1} = I_{m\times m}, \tag{26}$$

meaning the matrix $W\Phi_{m-1}$ is unitary, and thus $\kappa(W\Phi_{m-1}) = 1$, which is precisely the goal in numerically reliable identification as is described in Section 2.2. Furthermore, it follows from (25)–(26) that, for $k > m-1$, the last $k-(m-1)$ columns of Φ_k are all equal to zero, i.e., the polynomials $\phi_j(\xi)$ for $j > m-1$ have roots that coincide with all the nodes $\xi_1, \xi_2, \ldots, \xi_m$. This property is used in the following section to relate the set of polynomials to an upper-Hessenberg matrix containing recurrence coefficients.

3.2. Hessenberg recurrence matrix

Due to the strict degree constraint $\deg \phi_j(\xi) = j$, the polynomials $\{\phi_j(\xi)\}_{j=0}^k$ are all linearly independent. As a consequence, $\{\phi_j(\xi)\}_{j=0}^k$ form a basis for the space of all polynomials of degree less than or equal to k (Vandebril et al., 2008a, Chapter 12). In turn, this implies that the polynomial $\xi\phi_{k-1}(\xi)$ can be written as a linear combination of these polynomials, i.e.,

$$\xi\phi_{k-1}(\xi) = \sum_{j=0}^{k} \phi_j(\xi) h_{j,k-1}, \qquad k = 1, 2, 3, \ldots \tag{27}$$

where $h_{k,k-1} \neq 0$ since $\xi\phi_{k-1}(\xi)$ is of strict degree k. Given the recurrence coefficients, $h_{j,k}$, and ϕ_0, this relation can be used to recursively compute the full set of polynomials by rearranging (27) as

$$h_{k,k-1}\phi_k(\xi) = \xi\phi_{k-1}(\xi) - \sum_{j=0}^{k-1} \phi_j(\xi) h_{j,k-1}, \tag{28}$$

hence (27) and (28) are recurrence relations. Eq. (27) can be rewritten in matrix notation as

$$\xi \begin{bmatrix} \phi_0(\xi) & \cdots & \phi_{k-1}(\xi) \end{bmatrix} = \begin{bmatrix} \phi_0(\xi) & \cdots & \phi_k(\xi) \end{bmatrix} H_{(k+1)\times k}, \tag{29}$$

which, when evaluated at the nodes $\xi_1, \xi_2, \ldots, \xi_m$ that define the inner product (24), yields

$$X\Phi_{k-1} = \Phi_k H_{(k+1)\times k}, \tag{30}$$

with $X = \mathrm{diag}(\xi_1, \xi_2, \ldots, \xi_m)$. For $k = m$, the last column of Φ_m is equal to zero, as shown in Section 3.1, meaning (30) can be rewritten as,

$$X\Phi_{m-1} = \Phi_{m-1} H_{m\times m}. \tag{31}$$

Here, $H_{m\times m}$ is an upper-Hessenberg matrix containing the recurrence coefficients which, in conjunction with ϕ_0, can be used to compute $\{\phi_j(\xi)\}_{j=1}^{m-1}$.

3.3. Inverse eigenvalue problem

To relate nodes and weights defining the inner product (24) to the Hessenberg recurrence matrix, (31) is premultiplied by W,

$$W(X\Phi) = W(\Phi H), \tag{32}$$

where $\Phi = \Phi_{m-1}$ and $H = H_{m\times m}$ are used to simplify notation. Note that W and X commute due to their diagonal structure, hence (32) equals

$$X(W\Phi) = (W\Phi)H. \tag{33}$$

Since it follows from (26) that $Q = W\Phi$ is unitary, it follows from (33) that

$$Q^H X Q = H, \tag{34}$$

revealing that H is unitarily similar to X. Also, $Q\boldsymbol{e}_1$, the first column of $Q = W\Phi$ is equal to

$$Q\,\boldsymbol{e}_1 = W\phi_0 = \alpha \frac{\boldsymbol{w}}{\|\boldsymbol{w}\|_2}, \tag{35}$$

with $\boldsymbol{e}_1 = [1\ 0\ \cdots\ 0]^T$, $|\alpha| = 1$, and, $\boldsymbol{w}$ as defined in (11). The problem (34)–(35) is an inverse eigenvalue problem, where the desired Hessenberg recurrence matrix H has the nodes ξ_i as eigenvalues and the normalized weight vector $\boldsymbol{w}$ as the first eigenvector.

The inverse eigenvalue problem as given by (34)–(35) is not uniquely defined since each column of Q can be multiplied by a complex number of magnitude one without violating orthonormality. As an additional constraint, the sub-diagonal elements of H, as well as α in (35), are constrained to be positive real, thereby uniquely defining Q and H (Vandebril et al., 2008a, Chapter 12). To summarize, the inverse eigenvalue problem considered here is defined as follows.

Problem 1 (*Inverse Eigenvalue Problem*)**.** Given the nodes ξ_i and the weights w_i, $i = 1, 2, \ldots, m$, compute an upper Hessenberg matrix H, with subdiagonal elements $h_{k+1,k} \in \mathbb{R}_{>0}$, such that

- it is unitarily similar to the diagonal matrix $X = \mathrm{diag}(\xi_1, \xi_2, \ldots, \xi_m)$, i.e.,
  $$Q^H X Q = H,$$
- the first column of Q equals $\dfrac{\boldsymbol{w}}{\|\boldsymbol{w}\|_2}$, with $\boldsymbol{w}$ as in (11).

When Problem 1 has been solved, the recurrence relation (28) can subsequently be used to compute the orthonormal polynomial basis $\{\phi_j(\xi)\}_{j=0}^n$. The polynomial linear least-squares problem (10) is then solved by

$$\hat{\theta} = Q^H W \boldsymbol{y}, \tag{36}$$

$$\hat{p}(\xi_i, \hat{\theta}) = \Phi\hat{\theta}, \tag{37}$$

with $Q = W\Phi$, and W, Φ, and $\boldsymbol{y}$ as given by (16)–(17).

3.4. Update algorithm: chasing down the diagonal

To solve the inverse eigenvalue problem of Problem 1, a unitary matrix Q has to be determined such that

$$Q^H \left[\begin{array}{c|c|c} \boldsymbol{w} & X & \end{array}\right] \begin{bmatrix} 1 & \\ & Q \end{bmatrix} = \left[\begin{array}{c|c|c} \|\boldsymbol{w}\|_2\,\boldsymbol{e}_1 & H & \end{array}\right], \tag{38}$$

with $h_{k+1,k} \in \mathbb{R}_{>0}$.

An efficient method to solve this problem, as used in, e.g., Reichel, Ammar, and Gragg (1991), is to consider the update step, i.e., the problem of introducing a new node-weight pair to the problem which has been solved for the previously introduced node-weight pairs. This update step can be solved using Givens rotations, which are defined here as

$$[c, s, r] = G(a, b) \ \text{ s.t. } \begin{bmatrix} c & s \\ -s^* & c^* \end{bmatrix} \begin{bmatrix} a \\ b \end{bmatrix} = \begin{bmatrix} r \\ 0 \end{bmatrix}, \tag{39}$$

where $|c|^2 + |s|^2 = 1$, $a, b, c, s \in \mathbb{C}$ and $r \in \mathbb{R}^+$ (Bindel, Demmel, Kahan, & Marques, 2002). Here, the phase of r is constrained such that it is positive real, whereas conventionally Givens rotations are defined such that $c \in \mathbb{R}^+$. This choice reflects the choice to constrain the sub-diagonal elements of the Hessenberg recurrence matrix H to be positive real, as will be seen in the remainder of this section. To simplify the notation in the remainder of this section, a Givens rotation applied to two rows and/or columns is denoted as

$$\curvearrowright \begin{bmatrix} a \\ b \end{bmatrix} = \begin{bmatrix} c & s \\ -s^* & c^* \end{bmatrix} \begin{bmatrix} a \\ b \end{bmatrix} = \begin{bmatrix} r \\ 0 \end{bmatrix}. \tag{40}$$

When working with similarity transformations, as is the case in this paper, these transformations are always applied to two sides of the matrix. Here, the notation $\curvearrowright$ is used to denote the columns to which the Givens rotation is applied.

To perform the update step, a new node-weight pair $(\xi_i,\ w_i)$ is first added to the top of the augmented matrix $[\rho_{i-1}\,\boldsymbol{e}_1 \mid H_{o,i-1}]$, which has been brought to the desired form of (38) under unitary similarity. Here $\rho_{i-1} = \|\boldsymbol{w}_{i-1}\|_2$ where $\boldsymbol{w}_{i-1}$ is the vector containing weights $w_1, \ldots, w_{i-1}$. The new matrix $[\boldsymbol{w}_{n,i} \mid H_{n,i}]$ is given by

$$[\boldsymbol{w}_{n,i} \mid H_{n,i}] = \left[\begin{array}{c|cc} w_i & \xi_i & \\ \rho_{i-1}\,\boldsymbol{e}_1 & & H_{o,i-1} \end{array}\right], \tag{41}$$

where

$$[\boldsymbol{w}_{n,1} \mid H_{n,1}] = [w_1 \mid \xi_1]\,. \tag{42}$$

The matrix (41) is transformed to the form of (38) under unitary similarity, using Givens rotations. This is done by chasing the bulge element, i.e., the non-zero element which violates the desired matrix structure, down the diagonal using the following algorithm.

Algorithm 4 (*Chasing Down the Diagonal*)**.** A single update step is performed by first adding a new node-weight pair to obtain the augmented matrix as in (41). This matrix is then transformed to the form $[\rho_i\,\boldsymbol{e}_1 \mid H_{o,i}]$ under unitary similarity by the following operations. First, the second element in the weight vector is zeroed to transform it to the desired form of $\rho_i\boldsymbol{e}_1$, i.e.,

$$\left[\begin{array}{c|cccc} w_i & \xi_5 & & & \\ \rho_{i-1} & \times & \times & \times & \cdots \\ & \times & \times & \times & \cdots \\ & & \times & \times & \ddots \\ & & & \ddots & \ddots \end{array}\right] \Rightarrow \left[\begin{array}{c|cccc} \rho_i & \times & \times & \times & \cdots \\ 0 & \times & \times & \times & \cdots \\ & \star & \times & \times & \ddots \\ & & & \times & \ddots \\ & & & & \ddots \end{array}\right]. \tag{43}$$

This induces a non-zero element, denoted by $\star$, as the $(3,1)$ element of $\tilde{H}_i$, violating the Hessenberg structure. This element is subsequently zeroed by performing another Givens rotation

$$\left[\begin{array}{c|cccc} \rho_i & \times & \times & \times & \cdots \\ & \times & \times & \times & \cdots \\ & \star & \times & \times & \ddots \\ & & \times & \times & \ddots \\ & & & \ddots & \ddots \end{array}\right] \Rightarrow \left[\begin{array}{c|cccc} \rho_i & \times & \times & \times & \cdots \\ & \times & \times & \times & \cdots \\ & 0 & \times & \times & \ddots \\ & & \star & \times & \ddots \\ & & & \ddots & \ddots \end{array}\right], \tag{44}$$

which effectively moves the bulge element one step down the diagonal. This operation is repeated until the bulge element has been chased all the way down the diagonal where a final zeroing operation no longer introduces a new bulge element, i.e.,

$$\left[\begin{array}{c|cccc} \rho_i\boldsymbol{e}_1 & \ddots & \ddots & \ddots & \vdots \\ & \ddots & \times & \times & \times \\ & & \times & \times & \times \\ & & & \star & \times \end{array}\right] \Rightarrow \left[\begin{array}{c|cccc} \rho_i\boldsymbol{e}_1 & \ddots & \ddots & \ddots & \vdots \\ & \ddots & \times & \times & \times \\ & & \times & \times & \times \\ & & & 0 & \times \end{array}\right], \tag{45}$$

yielding the desired form $[\rho_i\,\boldsymbol{e}_1 \mid H_{o,i}]$.

Note that this sequence of Givens rotations, with the Givens rotations defined as in (39) with $r \in \mathbb{R}^+$, directly leads to $\rho_i \in \mathbb{R}^+$ and $h_{k+1,k} \in \mathbb{R}^+$. This update step needs to be performed for $i = 1, 2, \ldots, m$, to add each node-weight pair and, in each update step, $i-1$ rotations are performed operating on both columns and rows with at most i nonzero elements. This means the total computational cost of solving the inverse eigenvalue problem is $\mathcal{O}(m^3)$. In the case of polynomial least-squares problems where the orthonormal polynomial basis only needs to be built up to a limited polynomial degree n, the computational cost becomes $\mathcal{O}(mn^2)$, since only the first n rows and columns of the Hessenberg recurrence matrix need to be computed (Vandebril et al., 2008a, Section 12.5).

3.5. Special cases: matrix structure leading to an $\mathcal{O}(n)$ reduction in computational complexity

In the special case that all nodes ξ_i lie on the real line, the imaginary axis or the unit circle, the computational complexity of the inverse eigenvalue problem, Problem 1, can be reduced such that an update can be computed in $\mathcal{O}(n)$ operations instead of $\mathcal{O}(n^2)$. This is a result of additional structural properties of the Hessenberg recurrence matrix H which enable the Givens chasing operations described in Section 3.4 to be computed efficiently and also lead to a simplified recurrence relation (27).

3.5.1. Nodes on the real-line and imaginary axis

For the classical situation where $\xi_i \in \mathbb{R}$, the recurrence matrix H is Hermitian, since the diagonal node matrix satisfies $X^H = X$ and therefore

$$H^H = Q^H X^H Q = H\,. \tag{46}$$

This Hermitian Hessenberg matrix is tridiagonal and can be fully described using $\mathcal{O}(n)$ parameters, $\{a_i\}_{i=0}^n$ and $\{b_i\}_{i=1}^n$, as

$$H_{\mathcal{R}} = \begin{bmatrix} a_0 & b_1^* & & \\ b_1 & a_1 & \ddots & \\ & \ddots & \ddots & b_n^* \\ & & b_n & a_n \end{bmatrix}. \tag{47}$$

Furthermore, applying a Givens rotation to a tridiagonal matrix is an operation with a computational complexity of $\mathcal{O}(1)$, where it is $\mathcal{O}(n)$ for a full Hessenberg matrix, leading to the reduction of the computational complexity of the update algorithm described in Section 3.4 from $\mathcal{O}(n^2)$ to $\mathcal{O}(n)$. Also, it is immediate from (47) that the n-term recurrence relation (27) reduces to a three term recurrence relation,

$$\xi\phi_k(\xi) = b_k\phi_{k-1}(\xi) + a_k\phi_k(\xi) + b_{k+1}\phi_{k+1}(\xi)\,. \tag{48}$$

For the case where all ξ_i lie on the imaginary axis a similar situation occurs where the Hessenberg matrix is skew-Hermitian instead of Hermitian.

3.5.2. Nodes on the unit circle

In the case that all nodes ξ_i lie on the unit circle, the complex conjugate of each node is equal to its inverse since $\xi_i^{-1} = \frac{\xi_i^*}{|\xi_i|^2}$, and $|\xi_i| = 1$ for nodes on the unit circle. This means that for the diagonal node matrix

$$X^H = X^* = X^{-1}\,, \tag{49}$$

which leads to

$$H^H = Q^H X^H Q = H^{-1}\,, \tag{50}$$

meaning the Hessenberg recurrence matrix is unitary. This unitary Hessenberg matrix can again be fully described using $\mathcal{O}(n)$ parameters, $\{\gamma_i\}_{i=0}^n$ and $\{\sigma_i\}_{i=1}^n$, however this description is not

sparse as in the tridiagonal case, here

$$H_{\mathcal{T}} = \begin{bmatrix} -\gamma_0^*\gamma_1 & -\gamma_0^*\sigma_1\gamma_2 & -\gamma_0^*\sigma_1\sigma_2\gamma_3 & \cdots & -\gamma_0^*\sigma_{(1:n-1)}\gamma_n \\ \sigma_1 & -\gamma_1^*\gamma_2 & -\gamma_1^*\sigma_2\gamma_3 & \cdots & -\gamma_1^*\sigma_{(2:n-1)}\gamma_n \\ 0 & \sigma_2 & -\gamma_2^*\gamma_3 & \cdots & -\gamma_2^*\sigma_{(3:n-1)}\gamma_n \\ \vdots & \ddots & \ddots & \ddots & \vdots \\ 0 & \cdots & 0 & \sigma_{n-1} & -\gamma_{n-1}^*\gamma_n \end{bmatrix}, \tag{51}$$

where $\sigma_{(x:y)} = \prod_{i=x}^{y} \sigma_i$.

The key property of unitary Hessenberg matrices that leads to a reduction of the computational complexity is that unitary Hessenberg matrices can be written as a product of elementary unitary factors

$$H_{\mathcal{T}} = G_0' G_1 G_2 \dots G_{n-1} G_n', \tag{52}$$

with

$$G_0' = \gamma_0^* \oplus I_{n-1}, \qquad G_n' = I_{n-1} \oplus -\gamma_n, \tag{53}$$

$$G_k = I_{k-1} \oplus \begin{bmatrix} -\gamma_k & \sigma_k \\ \sigma_k & \gamma_k^* \end{bmatrix} \oplus I_{n-k-1}, \tag{54}$$

where $\oplus$ denotes the direct sum, i.e.,

$$A \oplus B = \begin{bmatrix} A & 0 \\ 0 & B \end{bmatrix}. \tag{55}$$

The representation (52) of unitary Hessenberg matrices is known as the Schur parametrization. As a result of this parametrization, the application of a single Givens rotation again has a computational complexity of $\mathcal{O}(1)$, due to the fact that only factors G_{k-1}, G_k and G_{k+1} are affected by an elementary similarity transformation operating on rows/columns k and $k+1$.

The unitary Hessenberg structure also leads to simplified recurrence relations. Indeed, these can be written as a two-term recurrence relation with a set of auxiliary polynomials $\{\tilde{\phi}(\xi)\}$,

$$\begin{bmatrix} \tilde{\phi}_0(\xi) \\ \phi_0(\xi) \end{bmatrix} = \frac{1}{\sigma_0} \begin{bmatrix} -\gamma_0^* \\ 1 \end{bmatrix}, \tag{56}$$

$$\begin{bmatrix} \tilde{\phi}_k(\xi) \\ \phi_k(\xi) \end{bmatrix} = \frac{1}{\sigma_k} \begin{bmatrix} 1 & -\gamma_k^* \\ -\gamma_k & 1 \end{bmatrix} \begin{bmatrix} \tilde{\phi}_{k-1}(x) \\ \xi\phi_{k-1}(x) \end{bmatrix}, \tag{57}$$

which is known as the Szegö recurrence relation. When $\gamma_k \neq 0 \; \forall \, k$, these relations can be rewritten as a three-term recurrence relation

$$\phi_{-1}(\xi) = 0, \qquad \phi_0(\xi) = \frac{1}{\sigma_0}, \tag{58}$$

$$\phi_k(\xi) = \frac{\phi_{k-1}(\xi)}{\sigma_k}\left(\xi + \frac{\gamma_k}{\gamma_{k-1}}\right) - \frac{\gamma_k}{\gamma_{k-1}}\frac{\sigma_{k-1}}{\sigma_k}\xi\phi_{k-2}(\xi), \tag{59}$$

further highlighting the similarity between the cases with nodes on the unit circle and with nodes on the real-line or imaginary axis as described in Section 3.5.1.

3.6. Towards a unified approach

In Sections 3.1–3.4, the theoretical framework of data-dependent orthonormal polynomials is established. It is shown that by solving an inverse eigenvalue problem, a Hessenberg recurrence matrix is constructed which uniquely determines the polynomial basis that is orthonormal with respect to the data-dependent inner product.

In Section 3.5, it is shown that there are additional structural properties for the Hessenberg recurrence matrix when the nodes that define the data-dependent inner product all lie on either the real-line, the imaginary axis or the unit circle. These structural properties lead to efficient construction algorithms for the discrete orthogonal polynomials, enabling the formulation of efficient and numerically reliable system identification approaches in both the continuous time Laplace domain, with nodes on the imaginary axis, and the discrete time Z-domain, with nodes on the unit circle.

From a system theoretical perspective, it indeed makes sense that similar structural properties exists for the Hessenberg recurrence matrix both in problems expressed in the continuous time Laplace domain and problems expressed in the discrete time Z-domain, since these are closely related. Indeed, through the use of invertible bilinear transformations several discrete time problems can be tackled with tools from continuous time system theory and *vice versa*, see, e.g., Iglesias and Glover (1991).

The general form of these bilinear transformations, known as Möbius transformations, is given by

$$\tilde{\xi} = \frac{\alpha\,\xi + \beta}{\mu\,\xi + \eta}, \tag{60}$$

with $\alpha,\ \beta,\ \mu,\ \eta \in \mathbb{C}$ and $\alpha\eta - \beta\mu \neq 0$. The full class of geometries that is related to the real-line and unit circle through Möbius transformations is the class of generalized circles, i.e., circles and lines, in the complex plane.

In the following section, the Möbius transformation is exploited to generalize the structural properties of the Hessenberg recurrence matrix that lead to a reduction in computational complexity to the case where all nodes lie on a generalized circle in the complex plane, including the real-line and unit-circle as special cases. This enables the fast construction of data-dependent orthonormal polynomials in the δ-domain without first transforming the problem to an equivalent Z-domain or s-domain formulation.

4. Orthogonal polynomials on generalized circles: a unified framework

In this section, the theoretical framework and algorithm are presented for the efficient construction of orthogonal polynomials with nodes on generalized circles in the complex plane. To extend the results of the real-line and unit circle cases, as described in Section 3.5, to generalized circles, their geometrical properties are investigated first in Section 4.1. Second, in Section 4.2 the structural properties of the Hessenberg recurrence matrix are investigated, resulting in a generalization of the structural properties as encountered in the real line and unit-circle cases for the generalized circle case. Next, in Section 4.3 it is shown how this generalized structure for the Hessenberg recurrence matrix again leads to an $\mathcal{O}(n)$ reduction in computational complexity as formulated in Theorem 14, this constitutes the first main result of this paper. Lastly, in Section 4.4 the construction algorithm is formulated in Algorithm 5, constituting the second main result of this paper.

4.1. Geometrical properties of generalized circles

The geometric properties of generalized circles are first defined and investigated, with a particular emphasis on their relation to the known real-line and unit circle cases. First, generalized circles are defined.

Definition 2 (*Generalized Circles*)**.** A generalized circle is a set of points ξ in the complex plane that satisfies the following equation

$$a\,\xi\xi^* + b\,\xi + c\,\xi^* + d = 0, \tag{61}$$

for any $a,\ d \in \mathbb{R}$ and $c,\ b \in \mathbb{C}$, such that $c = b^*$, and $ad < bc$, Schwerdtfeger (1979, Section 1.1).

Generalized circles are circles and straight lines in the complex plane and are therefore alternatively called clines or circlines. The general relation between two generalized circles is the Möbius transformation, (60), as defined in Section 3.6. In this section, a simplified version of the Möbius transformation is considered where no inversion is used, i.e., where $\mu = 0$, and $\eta = 1$. This simplified Möbius transformation can be considered as a composition of the following simple geometrical transformations: translation, homothety, and rotation (Schwerdtfeger, 1979). In the following lemma it is shown that all generalized circles can be transformed to the real-line or unit circle using this simplified Möbius transformation.

Lemma 3. *A set of nodes $\{\tilde{\xi}_i\}_{i=1}^m$ lies on a generalized circle in the unit plane if and only if $\exists\, c_1 \in \mathbb{C} \setminus \{0\}$, and $c_2 \in \mathbb{C}$, such that,*

$$\tilde{\xi}_i = c_1 \xi_i + c_2, \tag{62}$$

with $\xi_i \in \mathbb{R}\ \forall\ i$, or $|\xi_i| = 1\ \forall\ i$.

Proof. Applying transformation (62) to (61) yields,

$$a(c_1\xi + c_2)(c_1\xi + c_2)^* + b(c_1\xi + c_2) + c(c_1\xi + c_2)^* + d = 0. \tag{63}$$

When $a \neq 0$, taking $c_2 = -\frac{b}{a}$ and $c_1 = \sqrt{\frac{bc}{a^2} - \frac{d}{a}}$ yields

$$\left(\frac{bc}{a} - d\right)\xi\xi^* - \left(\frac{bc}{a} - d\right) = 0\,, \tag{64}$$

which corresponds to $\xi\xi^* = 1$, i.e., the unit circle. When $a = 0$, taking $c_2 = -\frac{d}{2}$ and $c_1 = jc$ yields

$$jbc\,\xi - jbc\,\xi^* = 0\,, \tag{65}$$

which corresponds to $\xi = \xi^*$, i.e., the real-line. The converse also holds since the transformation $\xi \mapsto \tilde{\xi}$ defined by (62) is invertible. □

Next, matrices that are unitarily similar to a diagonal node-matrix with nodes on a generalized circle are defined in the following as circline matrices.

Definition 4 (*Circline Matrices*)**.** A matrix $\tilde{U}$ is referred to as a circline matrix if it is unitarily similar to a diagonal matrix $\tilde{X} = \mathrm{diag}(\tilde{\xi}_1, \tilde{\xi}_2, \ldots, \tilde{\xi}_m)$, i.e.,

$$\tilde{U} = Q^H \tilde{X} Q\,, \tag{66}$$

with Q a unitary matrix, where the nodes $\{\tilde{\xi}_i\}_{i=1}^m$ lie on a generalized circle in the complex plane.

This class of matrices is important as it is the class of matrices encountered in the solution of the inverse eigenvalue problem (Problem 1) when the nodes lie on a generalized circle in the complex plane. The following Lemma shows the relation between the class of circline matrices and the unitary or Hermitian matrices encountered in the solution of the inverse eigenvalue problem in the unit circle and real line cases.

Lemma 5. *Let $\tilde{U} \in \mathbb{C}^{p\times p}$, be a circline matrix, then $\exists\, c_1 \in \mathbb{C} \setminus \{0\}$, and $c_2 \in \mathbb{C}$, such that,*

$$\tilde{U} = c_1 U + c_2 I\,, \tag{67}$$

where $U = Q^H X Q$ is a unitary or Hermitian matrix, with Q a unitary matrix and $X = \mathrm{diag}(\xi_1, \xi_2, \ldots, \xi_m)$ a diagonal node matrix with $\xi_i \in \mathbb{R}\ \forall\ i$, or $|\xi_i| = 1\ \forall\ i$.

Proof. From Definition 4,

$$\tilde{U} = Q^H \tilde{X} Q, \tag{68}$$

it follows from Lemma 3 that $\exists\, c_1 \in \mathbb{C}\setminus\{0\}$, and $c_2 \in \mathbb{C}$, such that,

$$\tilde{X} = c_1 X + c_2 I, \tag{69}$$

with $X = \mathrm{diag}(\xi_1, \xi_2, \ldots, \xi_m)$ a diagonal node matrix with $\xi_i \in \mathbb{R}\ \forall\ i$, or $|\xi_i| = 1\ \forall\ i$. Substituting (69) into (68) yields

$$\tilde{U} = Q^H(c_1 X + c_2 I)Q = c_1 U + c_2 I\,, \tag{70}$$

with $U = Q^H X Q$, as scalar-matrix multiplication is commutative and $Q^H I Q = I$. □

In Lemma 3 it is shown that a simple shifting and scaling operation (62) can be used to transform any generalized circle to either the real-line or the unit circle. Then, Lemma 5 essentially shows that this shifting and scaling operation commutes with unitary similarity transformations. As a result of this any circline matrix, as defined in Definition 4 and as encountered while solving the inverse eigenvalue problem (Problem 1) in the generalized circle case, can be written as a shifted and scaled version of a unitary or Hermitian matrix as are encountered in the real-line or the unit circle cases. This relationship between the matrices encountered in the generalized circle case and the matrices encountered in the real-line and unit circle cases is used in the next section to show that the structural properties of the Hessenberg recurrence matrix that lead to a reduction in computational complexity in the real-line and unit circle cases can be extended to the generalized circle case.

4.2. Structural properties of the Hessenberg recurrence matrix

To generalize the structural properties of the Hessenberg recurrence matrix, a class of structured matrices is investigated which contains both the tridiagonal matrices encountered in the real-line and imaginary axis cases as well as the unitary Hessenberg matrices encountered in the case with nodes on the unit circle. This class of matrices is called quasiseparable matrices (Bella, Eidelman, Gohberg, & Olshevsky, 2008), which is a type of rank-structured matrix. More specifically, the class of matrices investigated here is the class of Hessenberg-quasiseparable matrices with a separability rank of one, i.e., $(H,\ 1)$-quasiseparable matrices. Using the notation $A(i_1 : i_2, j_1 : j_2)$ to denote the submatrix of A containing rows i_1 to i_2 and columns j_1 to j_2, these $(H,\ 1)$-quasiseparable matrices are defined as follows.

Definition 6 (*$(H,\ 1)$-quasiseparable Matrices*)**.** An upper Hessenberg matrix H is $(H,\ 1)$-quasiseparable if,

$$\max_{1\leq i\leq n-1} \mathrm{rank}\,(H(1:i,\ i+1:n)) \leq 1\,. \tag{71}$$

The value of the rank constraint in (71), for all the blocks above the main diagonal, is known as the upper separability rank. This is defined here along with the lower separability rank as follows.

Definition 7 (*Separability Rank*)**.** Let $A \in \mathbb{C}^{n\times n}$, then A is quasiseparable with upper separability rank k_u, and lower separability rank k_l if

$$\max_{1\leq i\leq n-1} \mathrm{rank}\,(A(1:i,\ i+1:n)) \leq k_u\,, \tag{72}$$

$$\max_{1\leq i\leq n-1} \mathrm{rank}\,(A(i+1:n,\ 1:i)) \leq k_l\,. \tag{73}$$

The tridiagonal matrices encountered in the real-line case, i.e., (47), are indeed $(H,\ 1)$-quasiseparable as in this case the upper diagonal blocks are given by,

$$H_{\mathcal{R}}(1:i,\ i+1:n) = \begin{bmatrix} 0_{i-1\times 1} & 0_{i-1\times n-i} \\ b_i^* & 0_{1\times n-i} \end{bmatrix}, \tag{74}$$

which has one nonzero element and consequently its maximal rank is equal to one, as required in Definition 6. For the unitary Hessenberg matrices encountered in the unit-circle case, i.e., (51), the upper diagonal blocks are written as,

$$H_{\mathcal{T}}(1:i,\ i+1:n) = -\boldsymbol{a}^T\boldsymbol{b}, \tag{75}$$

where,

$$\begin{aligned} \boldsymbol{a} &= \begin{bmatrix} \gamma_0^*\sigma_{(1:i-1)} & \gamma_1^*\sigma_{(2:i-1)} & \cdots & \gamma_{i-2}^*\sigma_{i-1} & \gamma_{i-1}^* \end{bmatrix}, \\ \boldsymbol{b} &= \begin{bmatrix} \sigma_i\gamma_{i+1} & \sigma_i\sigma_{i+1}\gamma_{i+2} & \cdots & \sigma_{(i:n-1)}\gamma_n \end{bmatrix}, \end{aligned} \tag{76}$$

with $\sigma_{(x:y)} = \prod_{i=x}^{y}\sigma_i$. This shows that these upper diagonal blocks also have a maximal rank of one, showing that a unitary Hessenberg matrix is $(H,\ 1)$-quasiseparable.

Another property that is shared by both the unitary matrices encountered in the unit circle case and the Hermitian matrices encountered in the real-line case is that they are rank symmetric, as is shown in the following lemma.

Lemma 8 (*Rank Symmetry*). *Let U be a unitary or Hermitian $n\times n$ matrix. Then if U is lower quasiseparable with separability rank k it is also upper quasiseparable with the same rank.*

For a proof see Gemignani and Robol (2017, Theorem 5). In the following Theorem it is shown that this rank symmetry property can be extended to all circline matrices.

Theorem 9 (*Circline Rank Symmetry*). *Let $\tilde{U}\in\mathbb{C}^{n\times n}$ be a circline matrix. Then $\tilde{U}$ is rank symmetric, i.e., if $\tilde{U}$ is lower quasiseparable with separability rank k it is also upper quasiseparable with the same rank.*

Proof. Lemma 5 shows that $\tilde{U}$ can be written as

$$\tilde{U} = c_1U + c_2I, \tag{77}$$

where $U = Q^HXQ$ is a unitary or Hermitian matrix. As the quasiseparable rank-structure excludes the main diagonal, both the lower and the upper separability rank of $\tilde{U}$ is equal to that of c_1U. Therefore, as U is rank symmetric as a result of Lemma 8, $\tilde{U}$ is rank symmetric. □

Using this rank symmetry property, the following theorem shows that the class of Hessenberg recurrence matrices involved in the construction of a set of polynomials orthogonal with respect to a discrete inner-product with support on a generalized circle in the complex plane is indeed $(H,\ 1)$-quasiseparable.

Theorem 10. *Let $\tilde{H}\in\mathbb{C}^{n\times n}$ be a Hessenberg matrix that is also a circline matrix. Then $\tilde{H}$ is $(H,\ 1)$-quasiseparable.*

Proof. As $\tilde{H}$ is a Hessenberg matrix, its lower separability rank $h_l = 1$, as all blocks from below the main diagonal contain at most a single element. As $\tilde{H}$ is also a circline matrix, it is rank symmetric as a result of Theorem 9, therefore its upper separability rank $h_u = h_l = 1$, meaning $\tilde{H}$ is a $(H,\ 1)$-quasiseparable matrix. □

This key theoretical result shows that the Hessenberg recurrence matrices encountered in the generalized circle case indeed have the $(H,\ 1)$-quasiseparable structure. In the following section it is shown that this result, in conjunction with the rank symmetry result of Theorem 9, enables the efficient construction of orthogonal polynomials on generalized circles in the complex plane.

4.3. Efficient $\mathcal{O}(mn)$ construction of orthogonal polynomials on generalized circles

In the following section it is shown that the $(H,\ 1)$-quasiseparable matrix structure leads to a $\mathcal{O}(n)$ simplification of the construction algorithm for the orthonormal set of polynomials. For such an $\mathcal{O}(n)$ simplification to exist the following requirements must be met.

- R.1 The Hessenberg recurrence matrix $H\in\mathbb{C}^{n\times n}$ can be parametrized using $\mathcal{O}(n)$ parameters.
- R.2 There exist simplified recurrence relations that enable the computation of the orthonormal polynomial basis in $\mathcal{O}(mn)$ operations.
- R.3 The inverse eigenvalue problem as defined by Problem 1 can be solved in $\mathcal{O}(mn)$ operations.

The following lemma shows that an $(H,\ 1)$-quasiseparable matrix can be represented using $\mathcal{O}(n)$ generators.

Lemma 11 ($(H,\ 1)$-*quasiseparable Generators*). *Let $H\in\mathbb{C}^{n\times n}$ be a $(H,\ 1)$-quasiseparable matrix. Then H can be fully described with a set of generators $q_i,\ d_i,\ g_i,\ h_i,\ b_i,\ i=1,\ \ldots,\ n$, as follows*

$$H = \begin{bmatrix} d_1 & g_1h_2 & g_1b_2h_3 & \cdots & \cdots & g_1b_{(2:n-1)}h_n \\ q_1 & d_2 & g_2h_3 & \cdots & \cdots & g_2b_{(3:n-1)}h_n \\ 0 & q_2 & d_3 & \cdots & \cdots & g_3b_{(4:n-1)}h_n \\ \vdots & \ddots & \ddots & \ddots & \ddots & \vdots \\ \vdots & \ddots & \ddots & q_{n-2} & d_{n-1} & g_{n-1}h_n \\ 0 & \cdots & \cdots & 0 & q_{n-1} & d_n \end{bmatrix}, \tag{78}$$

where $b_{(x:y)} = \prod_{i=x}^{y} b_i$.

See Eidelman and Gohberg (1999, Theorem 3.5) for a proof. This description fulfills the first requirement R.1.

Furthermore, as shown in the following lemmas this generator description leads to the following simplified recurrence relations for the related polynomial systems.

Lemma 12 ($(H,\ 1)$-*quasiseparable 2-term r.r.*). *Let $H\in\mathbb{C}^{n\times n}$ be a $(H,\ 1)$-quasiseparable matrix described by a set of generators $q_i,\ d_i,\ g_i,\ h_i,\ b_i,\ i=1,\ \ldots,\ n$ as in (78). Then the set of polynomials $\{\phi_k(\xi)\}_{k=0}^n$ related to H through the n-term recurrence relation (29) can be obtained by the following 2-term block recurrence relation,*

$$\begin{bmatrix} F_0(\xi) \\ \phi_0(\xi) \end{bmatrix} = \begin{bmatrix} 0 \\ \alpha_0 \end{bmatrix}, \tag{79}$$

$$\begin{bmatrix} F_k(\xi) \\ \phi_k(\xi) \end{bmatrix} = \begin{bmatrix} \beta_k & \lambda_k \\ \delta_k & \alpha_k\xi+\varepsilon_k \end{bmatrix} \begin{bmatrix} F_{k-1}(\xi) \\ \phi_{k-1}(\xi) \end{bmatrix}, \tag{80}$$

where the conversion from the quasiseparable generators to the recurrence relation coefficients is given in Table 1.

Lemma 13 ($(H,\ 1)$-*quasiseparable 3-term r.r.*). *Let $H\in\mathbb{C}^{n\times n}$ be a $(H,\ 1)$-quasiseparable matrix described by a set of generators $q_i,\ d_i,\ g_i,\ h_i,\ b_i,\ i=1,\ \ldots,\ n$ as in (78), with $h_i\neq 0\ \forall\ i$. Then the set of polynomials $\{\phi_k(\xi)\}_{k=0}^n$ related to H through the n-term recurrence relation (29) can be obtained by the following 3-term recurrence relation,*

$$\phi_0(\xi) = \alpha_0, \quad \phi_1(\xi) = (\alpha_1\xi+\zeta_1)\cdot\phi_0(\xi), \tag{81}$$

$$\phi_k(\xi) = (\alpha_k\xi+\zeta_k)\cdot\phi_{k-1}(\xi) + (\eta_k\xi+\theta_k)\cdot\phi_{k-2}(\xi), \tag{82}$$

where the conversion from the quasiseparable generators to recurrence relation coefficients is given in Table 1.

Table 1
Conversion formulas from quasiseparable generators to recurrence relation coefficients.

Two-term block recurrence coefficients				
α_k	β_k	λ_k	δ_k	ε_k
$\frac{1}{q_k}$	b_k	$-g_k$	$\frac{h_k}{q_k}$	$-\frac{d_k}{q_k}$

Three-term recurrence coefficients			
α_k	ζ_k	η_k	θ_k
$\frac{1}{q_k}$	$\frac{h_k q_{k-1} b_{k-1} - d_k h_{k-1}}{q_k h_{k-1}}$	$-\frac{h_k b_{k-1}}{q_k h_{k-1}}$	$\frac{h_k (d_{k-1} b_{k-1} - h_{k-1} g_{k-1})}{q_k h_{k-1}}$

For proofs of Lemmas 12 and 13, and further details on these recurrence relations, see, e.g., Bella, Olshevsky, and Zhlobich (2011a, 2011b) and Eidelman, Gohberg, and Olshevsky (2005). The recurrence relations (79)–(82) fulfill requirement R.2.

Finally, the following theorem shows that the inverse eigenvalue problem can be solved with a reduced computational complexity when all nodes lie on a generalized circle. This theorem is the main result of this paper as it shows that the data-dependent orthonormal polynomials can be efficiently constructed in the generalized circle case.

Theorem 14. *Let the nodes $\{\tilde{\xi}_i\}_{i=1}^m$ all lie on a generalized circle in the complex plane. Then the inverse eigenvalue problem as defined by Problem 1 can be efficiently solved with a computational complexity of $\mathcal{O}(mn)$.*

Proof. All operations performed in Algorithm 4 are unitary similarity transformations. Therefore in all steps of the algorithm the matrix being operated on is a circline matrix as defined in Definition 4, since

$$\tilde{H}' = Q^H \tilde{X} Q, \tag{83}$$

with Q a unitary matrix and $\tilde{X} = \operatorname{diag}(\tilde{\xi}_i)$ where the nodes $\{\tilde{\xi}_i\}_{i=1}^m$ all lie on a generalized circle in the complex plane. As a result of Theorem 9 the matrix $\tilde{H}'$ is rank symmetric. When performing an update step, the problem matrix is Hessenberg apart from the one bulge element on the second subdiagonal that is being chased down. This bulge element does not increase the lower separability rank of the matrix as any matrix taken from below the main diagonal has either one of the following three structures

$$1: \begin{bmatrix} 0 & \times \\ 0 & 0 \end{bmatrix}, \quad 2: \begin{bmatrix} \star & \times \\ 0 & 0 \end{bmatrix}, \quad 3: \begin{bmatrix} 0 & \times \\ 0 & \star \end{bmatrix}, \tag{84}$$

which are all rank 1. Therefore, as a result of rank symmetry, the upper separability rank of $\tilde{H}'$ is also equal to one in all steps of the chasing algorithm. Performing a single chasing operation on the problem matrix thus means performing a Givens rotation on a matrix of the following structure,

$$G^H \tilde{H}' G = \begin{bmatrix} \ddots & \ddots & \vdots & \vdots & \vdots & \vdots & \vdots & \iddots \\ & \ddots & \times & \boxtimes & \boxtimes & \boxtimes & \boxtimes & \boxtimes & \cdots \\ & & \times & \times & \boxtimes & \boxtimes & \boxtimes & \boxtimes & \cdots \\ & & & \times & \times & \boxtimes & \boxtimes & \boxtimes & \cdots \\ & & & \star & \times & \times & \boxtimes & \boxtimes & \cdots \\ & & & & & \times & \times & \boxtimes & \cdots \\ & & & & & & \ddots & \ddots & \ddots \end{bmatrix}, \tag{85}$$

where $\boxtimes$ is used to denote the rank structured part of the matrix, i.e., any block out of this part of the matrix has a rank of one. Due to this rank structure, Performing a Givens rotation on the right $2 \times n$ part of the matrix, enclosed by the blue dash-dotted line, and top $n \times 2$ part, enclosed by the red dashed line, can be done with a computational complexity of $\mathcal{O}(1)$ instead of the general complexity $\mathcal{O}(n)$. As a result, Problem 1, can be solved with an overall computational complexity of $\mathcal{O}(mn)$ instead of $\mathcal{O}(mn^2)$ for the case where all nodes lie on a generalized circle in the complex plane. □

In the following section, the $(H, 1)$-quasiseparable matrix structure is employed to devise an efficient algorithm for chasing down the diagonal.

4.4. Update algorithm: chasing down the diagonal for $(H, 1)$-quasiseparable matrices

For notational simplicity the so-called well-free case is considered here where $h_i \neq 0 \ \forall \ i$, in which case it is possible to take $h_i = 1 \ \forall \ i$ without loss of generality, see, e.g., Bella et al. (2011a). This property generally holds in the context of system identification due to the stochastic nature of the identification data. In the following algorithm it is detailed how a single chasing operation of the chasing down the diagonal algorithm in Section 3.4 is performed for a $(H, 1)$-quasiseparable matrix with a computational complexity of $\mathcal{O}(1)$.

Algorithm 5 (*Chasing for $(H, 1)$-quasiseparable*)**.** A single chasing operation of the update algorithm of Section 3.4 is shown below acting on a $(H, 1)$-quasiseparable matrix $\tilde{H}'$ using the generator description of Lemma 11,

$G_i^H \tilde{H}'(i-1:i+5, i:i+4) G_i =$

$$\begin{bmatrix} g_{i-1} & g_{i-1}b_i & g_{i-1}b_{(i:i+1)} & g_{i-1}b_{(i:i+2)} & g_{i-1}b_{(i:i+3)} \\ d_i & g_i & g_i b_{i+1} & g_i b_{(i+1:i+2)} & g_i b_{(i+1:i+3)} \\ q_i & d_{i+1} & g_{i+1} & g_{i+1}b_{i+2} & g_{i+1}b_{(i+2:i+3)} \\ \star & q_{i+1} & d_{i+2} & g_{i+2} & g_{i+2}b_{i+3} \\ 0 & 0 & q_{i+2} & d_{i+3} & g_{i+3} \\ 0 & 0 & 0 & q_{i+3} & d_{i+4} \\ 0 & 0 & 0 & 0 & q_{i+4} \end{bmatrix} \tag{86}$$

The chasing operation performed on the middle part of $\tilde{H}'$, enclosed by the green dotted line in (86), leads to the following new values of the generators, denoted by the subscript n,

$$\begin{bmatrix} q_{i,n} & d_{i+1,n} & g_{i+1,n} \\ 0 & q_{i+1,n} & d_{i+2,n} \\ 0 & \star_n & q_{i+2,n} \end{bmatrix} \leftarrow \begin{bmatrix} q_i & d_{i+1} & g_{i+1} \\ \star & q_{i+1} & d_{i+2} \\ 0 & 0 & q_{i+2} \end{bmatrix}. \tag{87}$$

For the top part, enclosed by the red dashed line in (86), the following factorization can be made

$$\begin{bmatrix} \vdots & \vdots \\ g_{i-1}b_i & g_{i-1}b_{(i:i+1)} \\ g_i & g_i b_{i+1} \end{bmatrix} = \begin{bmatrix} \vdots \\ g_{i-1}\frac{b_i}{g_i} \\ 1 \end{bmatrix} \begin{bmatrix} g_i & b_{i+1}g_i \end{bmatrix}, \tag{88}$$

leading to the following new values of the generators,

$$g_{i,n} \leftarrow \begin{bmatrix} 1 & 0 \end{bmatrix} \begin{bmatrix} g_i & b_{i+1}g_i \end{bmatrix}, \tag{89}$$

$$b_{i+1,n} \leftarrow \begin{bmatrix} 0 & 1/g_{i,n} \end{bmatrix} \begin{bmatrix} g_i & b_{i+1}g_i \end{bmatrix}, \tag{90}$$

$$b_{i,n} \leftarrow g_{i,n} b_i / g_i. \tag{91}$$

Finally, for the right part, enclosed by the blue dash-dotted line in (86), the following factorization can be made

$$\begin{bmatrix} g_{i+1}b_{i+2} & g_{i+1}b_{(i+2:i+3)} & \cdots \\ g_{i+2} & g_{i+2}b_{i+3} & \cdots \end{bmatrix} = \begin{bmatrix} g_{i+1}b_{i+2} \\ g_{i+2} \end{bmatrix} \begin{bmatrix} 1 & b_{i+3} & \cdots \end{bmatrix}, \tag{92}$$

leading to the following new values of the generators,

$$\begin{bmatrix} b_{i+2,n} \\ g_{i+2,n} \end{bmatrix} \leftarrow \begin{bmatrix} 1/g_{i+1,n} & 0 \\ 0 & 1 \end{bmatrix} \begin{bmatrix} g_{i+1}b_{i+2} \\ g_{i+2} \end{bmatrix}. \tag{93}$$

After the replacements of the old generators with the new generators, i in (86) is increased by one and the same operation is performed again to chase the bulge one more step down the diagonal.

Here (91) is obtained from the fact that the factor b_i/g_i which appears in the column vector of the factorization in (88) must remain constant. Furthermore, the (2, 4)-element of the matrix in (86), which is not operated on, should also remain constant. This leads to the following additional condition that should be checked for Algorithm 5,

$$g_{i,n}b_{(i+1:i+2),n} = g_i b_{(i+1:i+2)}. \tag{94}$$

For the case of nodes on a generalized circle, this condition is guaranteed to hold due to the rank symmetry of circline matrices.

In the following section, this algorithm is used to obtain a unified framework for numerically reliable identification in the Laplace domain, the Z-domain and the δ-domain.

5. Identification approach and implementation aspects

In this section the results from Section 4 are applied to obtain a unified framework for numerically reliable system identification.

5.1. Unified identification approach

The unified identification approach as proposed in this paper is summarized in Fig. 2. In particular, it is shown how, starting with FRF data of a given system, a system model is identified using a class of well-known identification algorithms in combination with numerically optimal polynomial basis functions expressed in either the Laplace domain, the Z-domain or δ-domain.

Remark 15. Determining the appropriate model order is a part of the general identification problem. The proposed identification approach requires the user to select the maximum degree of the approximant in the polynomial least-squares problem. However, as the data-dependent orthonormal polynomial approach recursively builds up the orthonormal polynomial basis, it becomes trivial to also obtain all the lower order approximations, see, e.g., Pintelon and Kollár (2005). This enables the subsequent determination of the appropriate model order by, e.g., applying a statistical information criterion or by plotting and analyzing the stabilization diagram.

Remark 16. When the computed matrix $Q = W\Phi$ is not sufficiently unitary, as determined by some user-defined metric, e.g., if $\kappa(Q) > 1 + \varepsilon_{\text{tol}}$ for some tolerance ε_{tol}, then an additional re-orthogonalization step can be performed by explicitly solving the over-determined system of Eqs. (15) using a standard solver, e.g., a QR-solver, instead of using (36)–(37).

A requirement for the implementation of the proposed approach for system identification, is that the obtained solution polynomials are real-valued. How to make sure real-valued polynomials are obtained, is considered next.

5.2. Real-valued polynomials

To make sure the obtained polynomials are real-valued, the discrete inner product needs to be defined such that all the node-weight pairs are added in conjunction with their complex conjugates. To do this, the weight vector $\boldsymbol{w}$ and node matrix X are

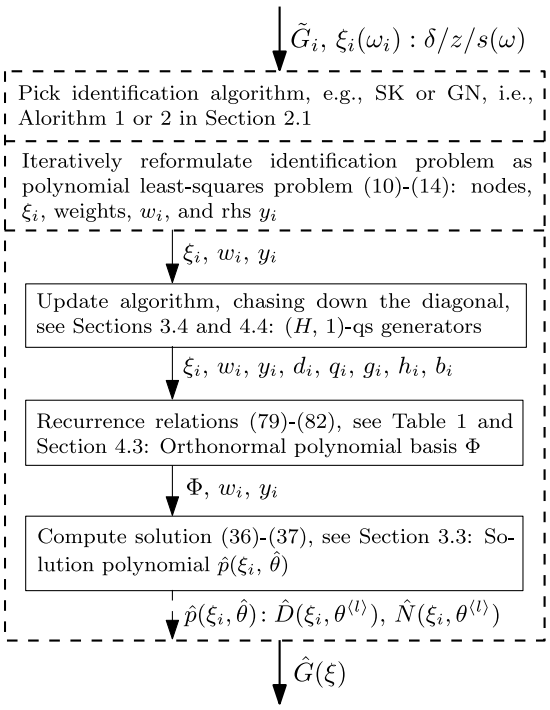

Fig. 2. Unified numerically reliable identification approach.

extended to include all the complex conjugate nodes and weights as follows,

$$\boldsymbol{w}_c = \begin{bmatrix} w_1 & w_1^* & \cdots & w_m & w_m^* \end{bmatrix}^T, \tag{95}$$

$$X_c = \operatorname{diag}\left(\begin{bmatrix} \xi_1 & \xi_1^* & \cdots & \xi_m & \xi_m^* \end{bmatrix}\right). \tag{96}$$

When adding the node-weight pairs as in (95)–(96), then after every second update step of the algorithm in Section 4.4, i.e., when a complex conjugate pair has been added, the $(H,\ 1)$-quasiseparable generators are all real apart from possible numerical errors. Therefore after every second update step all imaginary parts of the generators can be set to zero. Even though this approach does not fully utilize the conjugate symmetry inherent in the problem to maximally reduce the computational complexity, it is sufficiently efficient and numerically reliable for the purposes of this paper.

An effective approach to utilize the conjugate symmetry inherent in the problem is the chasing two-down the diagonal approach, as described in, e.g, van Herpen et al. (2016). In this approach, the node-weight pairs are again added as in (95)–(96) and then the following transformation is performed

$$T_0 = \frac{1}{\sqrt{2}} I_m \otimes \begin{bmatrix} 1 & j \\ 1 & -j \end{bmatrix}, \tag{97}$$

$$\begin{aligned} \boldsymbol{w}_r &= T_0^H \boldsymbol{w}_c \\ &= \sqrt{2}\begin{bmatrix} \operatorname{Re}(w_1) & \operatorname{Im}(w_1) & \cdots & \operatorname{Re}(w_m) & \operatorname{Im}(w_m) \end{bmatrix}^T, \end{aligned} \tag{98}$$

$$\begin{aligned} X_r &= T_0^H X_c T_0 \\ &= \begin{bmatrix} \operatorname{Re}(\xi_1) & -\operatorname{Im}(\xi_1) \\ \operatorname{Im}(\xi_1) & \operatorname{Re}(\xi_1) \end{bmatrix} \oplus \cdots \oplus \begin{bmatrix} \operatorname{Re}(\xi_m) & -\operatorname{Im}(\xi_m) \\ \operatorname{Im}(\xi_m) & \operatorname{Re}(\xi_m) \end{bmatrix}. \end{aligned} \tag{99}$$

After this transformation is performed all calculations can be performed on real coefficients, effectively leading to a factor two reduction in computational complexity. However, in this chasing two-down approach, a block of two node-weight pairs, each others complex conjugates, has to be added and chased down the diagonal in conjunction. This leads to a larger non-trivial

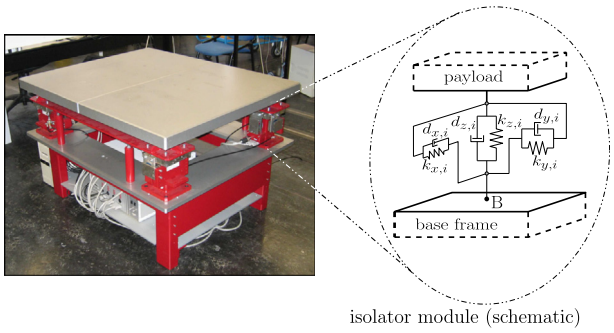

Fig. 3. The AVIS setup and a schematic representation of one of the four isolator modules.

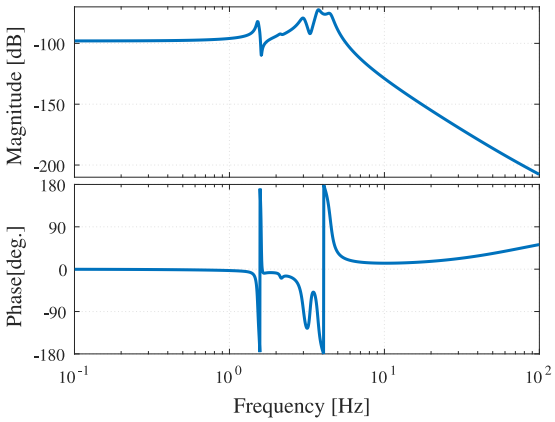

Fig. 4. Bode-diagram of the simulation model, based on a rigid-body AVIS model from moment M_x to rotation θ_y.

block on which to perform the calculations since simultaneously adding two bulge elements below the first sub-diagonal of the Hessenberg matrix does increase the rank of the corresponding lower diagonal blocks, which due to rank symmetry will also cause the upper diagonal blocks to become rank 2. Therefore the chasing two-down approach is not used in this paper and its implementation for the quasiseparable Hessenberg matrix case is considered as future work.

6. Example

In this section the numerical advantages of the proposed approach are shown using a simulation example.

6.1. System description

In this section an Active Vibration Isolation System (AVIS) is considered as is shown in Fig. 3. The system is modeled as a rigid isolated payload connected to a rigid base frame with four isolator modules as detailed in Beijen, Voorhoeve, Heertjes, and Oomen (2018). The example considered in this paper is based on the SISO transfer function between a moment M_x, applied to the payload in the θ_x direction and the resulting rotation in the θ_y direction. The Bode diagram of this transfer function is shown in Fig. 4. This is a relevant case study in the context of the present paper, as the sampling frequency used is often much higher than the dominant dynamics for such a system.

6.2. Methods

The true system $G_0(\xi)$ is given by

$$G_0(\xi) = \frac{n_0(\xi)}{d_0(\xi)}. \tag{100}$$

In this simulation example, the denominator polynomial $d_0(\xi)$ is estimated from simulated FRF data of the system, $\tilde{G}(\xi_i)$, and it is assumed that the true numerator polynomial $n_0(\xi)$ is known. This is done to reduce the identification problems problem to a scalar polynomial least-squares problem as is considered in this paper. The vector polynomial case that is encountered when jointly estimating $d_0(\xi)$ and $n_0(\xi)$ with optimal numerical conditioning, as in Bultheel et al. (2005), is not considered further here, but follows along the same lines as is explained in Section 7.

The simulated FRF data $\tilde{G}(\omega_i)$ is given as,

$$\tilde{G}(\omega_i) = G_0(\xi_i) + \nu_i, \tag{101}$$

where ν_i is randomly generated, circularly complex normally distributed noise with zero mean and a variance which is constant for all i with a value of 0.1 times the median absolute value of $G_0(\xi_i)$. In this example 10^3 frequency points, ω_i, are considered which are logarithmically spaced between 0.5 and 10 Hz.

To identify the denominator polynomial from this data, ten iterations of the SK-algorithm, Algorithm 2, are used where $\hat{n}(\xi_i, \theta)$ is replaced with $n_0(\xi_i)$ and where $\hat{d}(\xi_i, \theta^{(0)}) = 1$. This identification procedure is performed using three different approaches. First, in the Z-domain using the Schur parametrization of Section 3.5.2 to represent the Hessenberg recurrence matrix, implemented as a rotation-chasing algorithm similar to Vandebril (2011). Second, in the Z-domain using the presented approach of Section 5 where the computations are performed on the quasiseparable generators that represent the Hessenberg recurrence matrix. Third, in the δ-domain, also using the proposed approach of Section 5.

These three identification approaches are all implemented and performed for increasing sampling frequencies in single precision floating-point arithmetic. To compare the performance of the approaches, two metrics are used, first is the conditioning of the matrix $Q = W\Phi$, which should be equal to 1 when the orthogonalization procedure is successful. To quantify the orthogonalization performance, the geometric mean of $\kappa(Q) - 1$ over all iterations is considered, i.e.,

$$\mu_g\{\kappa(Q) - 1\} = \prod_{l=1}^{10} \left(\kappa(Q^{\langle l \rangle}) - 1\right)^{1/10}. \tag{102}$$

As a second metric the converged cost function is considered which is determined here as the arithmetic mean of cost function values of the last three iterations, i.e.,

$$V_{\text{conv}} = \frac{1}{3} \sum_{l=8}^{10} V^{\langle l \rangle}, \tag{103}$$

where,

$$V^{\langle l \rangle} = \sum_{i=1}^{m} \left| w_i \left(\tilde{G}(\xi_i) - \frac{n_0(\xi_i)}{\hat{d}(\xi_i, \theta^{\langle l \rangle})} \right) \right|^2. \tag{104}$$

Whenever an invalid number, i.e., $\pm\infty$ or NaN, is encountered it is replaced by the maximum conditioning number for determining $\mu_g\{\kappa(Q) - 1\}$ and for determining V_{conv} the last three valid values for $V^{\langle l \rangle}$ are used.

6.3. Results

In this section, the results are presented for the AVIS example. First, the results related to the conditioning of the matrix $Q = W\Phi$ are presented. Next, the results for the converged cost function values are presented.

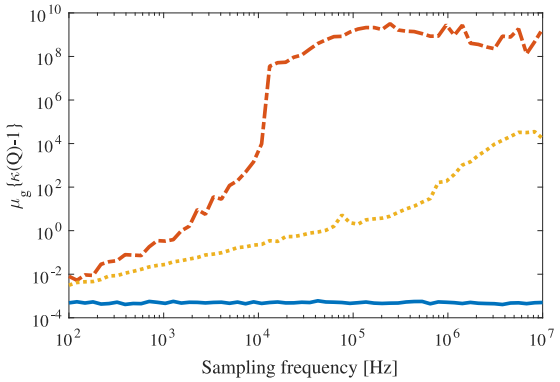

Fig. 5. Conditioning results $\mu_g\{\kappa(Q)-1\}$ for different sampling frequencies without re-orthogonalization. Shows that the conditioning numbers for the Z-domain approaches with the Schur parametrization (red dash-dotted) and the quasiseparable parametrization (yellow dotted) increase with increasing sampling frequency and are much higher than those for the δ-domain approach proposed in this paper (blue solid) where the conditioning numbers remain close to optimal $\kappa = 1$ for all sampling frequencies.

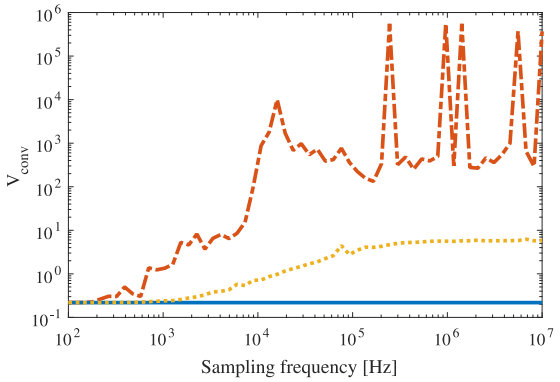

Fig. 6. Converged cost results for different sampling frequencies without re-orthogonalization. Shows that for high sampling frequencies the Z-domain approaches with the Schur parametrization (red dash-dotted) and the quasiseparable parametrization (yellow dotted) are no longer able to reach a low cost function value while the δ-domain approach proposed in this paper (blue solid) reaches the same low cost function value for all sampling frequencies.

6.3.1. Conditioning results

In Fig. 5, the conditioning results are shown for different sampling frequencies. These results can be interpreted as a measure for the numerical loss of significance in the orthogonalization procedure. From this figure it is clear that the numerical performance of the δ-domain approach is superior to that of both Z-domain approaches. For the δ-domain approach, the numerical performance is independent of the sampling frequency while for both Z-domain approaches the numerical performance deteriorates with increasing sampling frequency.

Closer inspection reveals that for the Z-domain approach with the Schur parametrization the numerical loss of significance initially scales quadratically with the sampling frequency while for the Z-domain approach with the quasiseparable parametrization this scaling is linear. After this initial scaling, a sharp increase in the numerical loss of significance can be observed once $\kappa(Q) - 1 > 1$, which can be viewed as a sort of threshold after which orthogonality is lost. The observed difference in initial scaling for the two Z-domain approaches can be explained from the fact that in the quasiseparable parametrization the main diagonal is linearly parametrized as d_i, while the main diagonal in the Schur parametrization is parametrized quadratically as $\gamma_{i-1}^* \gamma_i$.

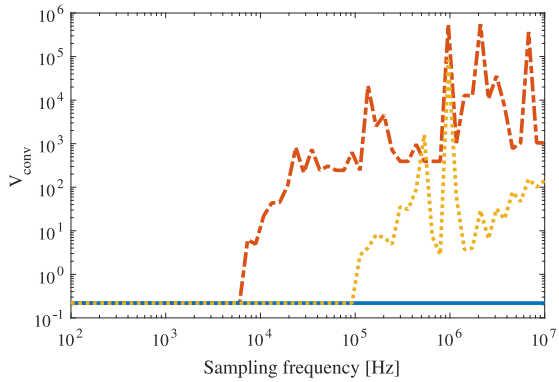

Fig. 7. Converged cost results for different sampling frequencies with re-orthogonalization. Shows that re-orthogonalization can be used to extend the range of sampling frequencies for which the Z-domain approaches with the Schur parametrization (red dash-dotted) and the quasiseparable parametrization (yellow dotted) are able to reach a low cost function value but that these approaches still break down for higher sampling frequencies while the δ-domain approach proposed in this paper (blue solid) reaches the same low cost function value for all sampling frequencies.

6.3.2. Converged cost results

The converged cost function values are depicted in Figs. 6 and 7, which respectively show the results using no re-orthogonalization, as described in Remark 16, and the results where re-orthogonalization is used. In these figures it can be seen that for the lowest sampling frequencies all the considered approaches in Z-domain and δ-domain lead to the same cost function values. This should be the case since, apart from the numerical properties, the considered approaches are equivalent and should yield the same results. For the case without re-orthogonalization, as depicted in Fig. 6, the cost function values start to diverge at relatively low values of the sampling frequency. It is observed that the performance of the Z-domain approach using the Schur parametrization starts to deteriorate first around a sampling frequency of 300 Hz. The Z-domain approach using the quasiseparable parametrization starts to show performance degradation from a sampling frequency of 1 kHz. The δ-domain approach proposed in this paper shows no degradation in performance as the sampling frequency increases.

From Fig. 7, it is observed that re-orthogonalization can help to increase the range of sampling frequencies for which the performance of both Z-domain approaches does not deteriorate. However, this does not solve the underlying numerical issues, but merely mitigates their effects. For the purpose of obtaining a numerically reliable identification approach, this re-orthogonalization step therefore does not add much. It is clear from these results that the proposed δ-domain approach does solve the underlying numerical challenges that exists for the identification of fast sampled systems in discrete time.

7. Conclusions and outlook

This paper has brought together the aspects of orthonormal polynomials with respect to data-dependent inner products and δ-domain formulations in systems and control, thereby providing a new unified view on the numerically reliable implementation of algorithms in system identification and control. This is applied to develop a unified approach for numerically reliable system identification where identification in Laplace domain, Z-domain and δ-domain are all incorporated as special cases. In Section 6, an example based on a Active Vibration Isolation System is presented, the results of which show that the developed δ-domain

approach is numerically superior to the alternative Z-domain approaches.

It is considered ongoing research to extend the presented unified numerically reliable identification approach from the scalar polynomial case to the vector polynomial case for the identification of rational and MIMO system models. This will likely involve extending the scalar quasiseparable generator description to a block-generator description as in, e.g., Vandebril, Van Barel, and Mastronardi (2008b, Chapter 12) and adjusting the chasing operations accordingly to accommodate this block-quasiseparable structure.

Acknowledgments

This research is supported by the TU/e impulse program in collaboration with ASML Research and is part of the research programme VIDI with project number 15698, financed by the Netherlands Organization for Scientific Research (NWO).

References

Ammar, G., Gragg, W., & Reichel, L. (1991). Constructing a unitary Hessenberg matrix from spectral data. In G. H. Golub, & P. Van Dooren (Eds.), *Numerical linear algebra, digital signal processing and parallel algorithms* (pp. 385–395). Berlin, Heidelberg: Springer Berlin Heidelberg.

Van der Auweraer, H., Guillaume, P., Verboven, P., & Vanlanduit, S. (2001). Application of a fast-stabilizing frequency domain parameter estimation method. *Transactions of the ASME. Journal of Dynamic Systems, Measurement and Control*, *123*(4), 651–658.

Bayard, D. S. (1994). High-order multivariable transfer function curve fitting: Algorithms, sparse matrix methods and experimental results. *Automatica*, *30*(9), 1439–1444.

Beijen, M. A., Voorhoeve, R., Heertjes, M. F., & Oomen, T. (2018). Experimental estimation of transmissibility matrices for industrial multi-axis vibration isolation systems. *Mechanical Systems and Signal Processing*.

Bella, T., Eidelman, Y., Gohberg, I., & Olshevsky, V. (2008). Computations with quasiseparable polynomials and matrices. In *symbolic-Numerical Computations Theoretical Computer Science*, *409*(2), 158–179.

Bella, T., Olshevsky, V., & Zhlobich, P. (2011a). *Classifications of recurrence relations via subclasses of (H, m)-quasiseparable matrices* (pp. 23–53). Dordrecht: Springer Netherlands.

Bella, T., Olshevsky, V., & Zhlobich, P. (2011b). A quasiseparable approach to five-diagonal CMV and Fiedler matrices. *Linear Algebra and its Applications*, *434*(4), 957–976.

Benner, P. (2004). Solving large-scale control problems. *IEEE Control Systems*, *24*(1), 44–59.

Bindel, D., Demmel, J., Kahan, W., & Marques, O. (2002). On computing givens rotations reliably and efficiently. *ACM Transactions on Mathematical Software*, *28*(2), 206–238.

Bultheel, A., & Barel, M. V. (1995). Vector orthogonal polynomials and least squares approximation. *SIAM Journal of Mathematical Analysis*, *16*(3), 863–885.

Bultheel, A., Barel, M. V., Rolain, Y., & Pintelon, R. (2005). Numerically robust transfer function modeling from noisy frequency domain data. *IEEE Transactions on Automatic Control*, *50*(11), 1835–1839.

Collins, E. G., Jr., & Song, T. (1999). A delta operator approach to discrete-time h_∞ control. *International Journal of Control*, *72*(4), 315–320.

Datta, B. N. (2004). *Numerical methods for linear control systems: Design and analysis, vol. 1*. Academic Press.

Eidelman, Y., & Gohberg, I. (1999). On a new class of structured matrices. *Integral Equations Operator Theory*, *34*(3), 293–324.

Eidelman, Y., Gohberg, I., & Olshevsky, V. (2005). Eigenstructure of order-one-quasiseparable matrices. Three-term and two-term recurrence relations. *Linear Algebra and its Applications*, *405*, 1–40.

Gautschi, W. (1983). The condition of Vandermonde-like matrices involving orthogonal polynomials. *Linear Algebra and its Applications*, *52*, 293–300.

Gautschi, W. (2004). Orthogonal polynomials: Computation and approximation. In *Numerical mathematics and scientific computation*, Oxford University Press.

Gemignani, L., & Robol, L. (2017). Fast Hessenberg reduction of some rank structured matrices. *SIAM Journal of Mathematical Analysis*, *38*(2), 574–598.

Gevers, M., & Li, G. (1993). *Parametrizations in the delta operator* (pp. 289–318). London: Springer London.

Gilson, M., Welsh, J. S., & Garnier, H. (2018). A frequency localizing basis function-based IV method for wideband system identification. *IEEE Transactions on Control Systems Technology*, *26*(1), 329–335.

Goodwin, G. C., Graebe, S. F., & Salgado, M. E. (2000). *Control system design* (1st ed.). Upper Saddle River, NJ, USA: Prentice Hall PTR.

Goodwin, G., Leal, R., Mayne, D., & Middleton, R. (1986). Rapprochement between continuous and discrete model reference adaptive control. *Automatica*, *22*(2), 199–207.

Goodwin, G. C., Middleton, R. H., & Poor, H. V. (1992). High-speed digital signal processing and control. *Proceedings of the IEEE*, *80*(2), 240–259.

Gragg, W. B., & Harrod, W. J. (1984). The numerically stable reconstruction of Jacobi matrices from spectral data. *Numerische Mathematik*, *44*(3), 317–335.

Gustavsen, B., & Semlyen, A. (1999). Rational approximation of frequency domain responses by vector fitting. *IEEE Transactions on Power Delivery*, *14*(3), 1052–1061.

van Herpen, R., Bosgra, O., & Oomen, T. (2016). Bi-orthonormal polynomial basis function framework with applications in system identification. *IEEE Transactions on Automatic Control*, *61*(11), 3285–3300.

van Herpen, R., Oomen, T., & Steinbuch, M. (2014). Optimally conditioned instrumental variable approach for frequency-domain system identification. *Automatica*, *50*(9), 2281–2293.

Iglesias, P., & Glover, K. (1991). State-space approach to discrete-time $\mathcal{H}_\infty$ control. *International Journal of Control*, *54*(5), 1031–1073.

Levy, E. C. (1959). Complex-curve fitting. *IRE Transactions on Automatic Control*, *AC-4*(1), 37–43.

Li, G., & Gevers, M. (1993). Comparative study of finite word length effects in shift and delta operator parameterizations. *IEEE Transactions on Automatic Control*, *38*(5), 803–807.

Middleton, R., & Goodwin, G. (1986). Improved finite word length characteristics in digital control using delta operators. *IEEE Transactions on Automatic Control*, *31*(11), 1015–1021.

Ninness, B., & Hjalmarsson, H. (2001). Model structure and numerical properties of normal equations. *IEEE Transactions on Circuits and Systems I*, *48*(4), 425–437.

Oomen, T., van Herpen, R., Quist, S., van de Wal, M., Bosgra, O., & Steinbuch, M. (2014). Connecting system identification and robust control for next-generation motion control of a wafer stage. *IEEE Transactions on Control Systems Technology*, *22*(1), 102–118.

Pintelon, R., & Kollár, I. (2005). On the frequency scaling in continuous-time modeling. *IEEE Transactions on Instrumentation and Measurement*, *54*(1), 318–321.

Pintelon, R., Rolain, Y., Bultheel, A., & Barel, M. V. (2004). Frequency domain identification of multivariable systems using vector orthogonal polynomials. In *Proceedings of the 16th international symposium on mathematical theory of networks and systems*.

Pintelon, R., & Schoukens, J. (2012). *System identification: A frequency domain approach* (2nd ed.). Hoboken, NJ, USA: Wiley-IEEE press.

Reichel, L., Ammar, G. S., & Gragg, W. B. (1991). Discrete least squares approximation by trigonometric polynomials. *Mathematics of Computation*, *57*(195), 273.

Rolain, Y., Pintelon, R., Xu, K., & Vold, H. (1995). Best conditioned parametric identification of transfer function models in the frequency domain. *IEEE Transactions on Automatic Control*, *40*(11), 1954–1960.

Sanathanan, C. K., & Koerner, J. (1963). Transfer function synthesis as a ratio of two complex polynomials. *IEEE Transactions on Automatic Control*, *8*(1), 56–58.

Schwerdtfeger, H. (1979). Geometry of complex numbers. In *Dover books on mathematics*, Dover Publications.

Simon, B. (2005). *Orthogonal polynomials on the unit circle, vol. 54*. American Mathematical Society.

Suchomski, P. (2001). Numerical conditioning of delta-domain Lyapunov and Riccati equations. *IEE Proceedings D (Control Theory and Applications)*, *148*, 497–501.

Szegö, G. (1939). *Orthogonal polynomials, vol. 23*. American Mathematical Society.

Vandebril, R. (2011). Chasing bulges or rotations? A metamorphosis of the QR-algorithm. *SIAM Journal of Mathematical Analysis*, *32*(1), 217–247.

Vandebril, R., Van Barel, M., & Mastronardi, N. (2008a). *Matrix computations and semiseparable matrices: Eigenvalue and singular value methods (volume 2)*.

Vandebril, R., Van Barel, M., & Mastronardi, N. (2008b). *Matrix computations and semiseparable matrices: Linear systems (volume 1)*.

Varga, A. (2004). Numerical awareness in control. *IEEE Control Systems*, *24*(1), 14–17.

Voorhoeve, R., & Oomen, T. (2018). Numerically reliable identification of fast sampled systems: A novel δ-domain data-dependent orthonormal polynomial approach. In *57th IEEE conference on decision and control* (pp. 1433–1438).

Voorhoeve, R., van Rietschoten, A., Geerardyn, E., & Oomen, T. (2015). Identification of high-tech motion systems: An active vibration isolation benchmark. In *17th IFAC symposium on system identification* (pp. 1250–1255). Beijing, China.

Voorhoeve, R., de Rozario, R., & Oomen, T. (2016). Identification for motion control: Incorporating constraints and numerical considerations. In *2016 American control conference* (pp. 6209–6214). Boston, MA, USA.

Wahlberg, B., & Mäkilä, P. (1996). On approximation of stable linear dynamical systems using Laguerre and Kautz functions. *Automatica, 32*(5), 693–708.
Welsh, J. S., & Goodwin, G. C. (2003). Frequency localising basis functions for wide-band identification. In *2003 European control conference* (pp. 376–381). Cambridge, UK.
Yang, H., Xia, Y., Shi, P., & Zhao, L. (2012). *Analysis and synthesis of delta operator systems, vol. 430*. Springer.

Robbert Voorhoeve received the M.Sc. degree in Mechanical Engineering (cum laude) and Applied Physics in 2013 and his Ph.D. degree in 2018 from the Eindhoven University of Technology, Eindhoven, The Netherlands. His research interests include system identification, identification for advanced motion control, and control of complex mechatronic systems.

Tom Oomen received the M.Sc. degree (cum laude) and Ph.D. degree from the Eindhoven University of Technology, Eindhoven, The Netherlands. He is currently a professor with the Department of Mechanical Engineering at the Eindhoven University of Technology. He held visiting positions at KTH, Stockholm, Sweden, and at The University of Newcastle, Australia. He is a recipient of the Corus Young Talent Graduation Award, the IFAC 2019 TC 4.2 Mechatronics Young Research Award, the 2015 IEEE Transactions on Control Systems Technology Outstanding Paper Award, the 2017 IFAC Mechatronics Best Paper Award, the 2019 IEEJ Journal of Industry Applications Best Paper Award, and recipient of a Veni and Vidi personal grant. He is Associate Editor of the IEEE Control Systems Letters (L-CSS), IFAC Mechatronics, and IEEE Transactions on Control Systems Technology. He is a member of the Eindhoven Young Academy of Engineering. His research interests are in the field of data-driven modeling, learning, and control, with applications in precision mechatronics.